



Studying the dynamics and the structure of Gamma-Ray Bursts with the VLBI

Speaker

S. Giarratana

Supervisor

Dr. M. Giroletti

Collaborators

Prof G. Ghirlanda, Dr. O.S. Salafia, Dr. L. Rhodes, Dr. B. Marcote, Dr. M.E. Ravasio and many more...

Long and Short

$T_{90} \geq 2s$
(Kouveliotou+93)

$\langle z \rangle \simeq 2.0$
(Berger13,...)

High star-forming regions
(Berger09, Fong+13, Berger13,...)

Associated with SNe
(Galama+98,...)



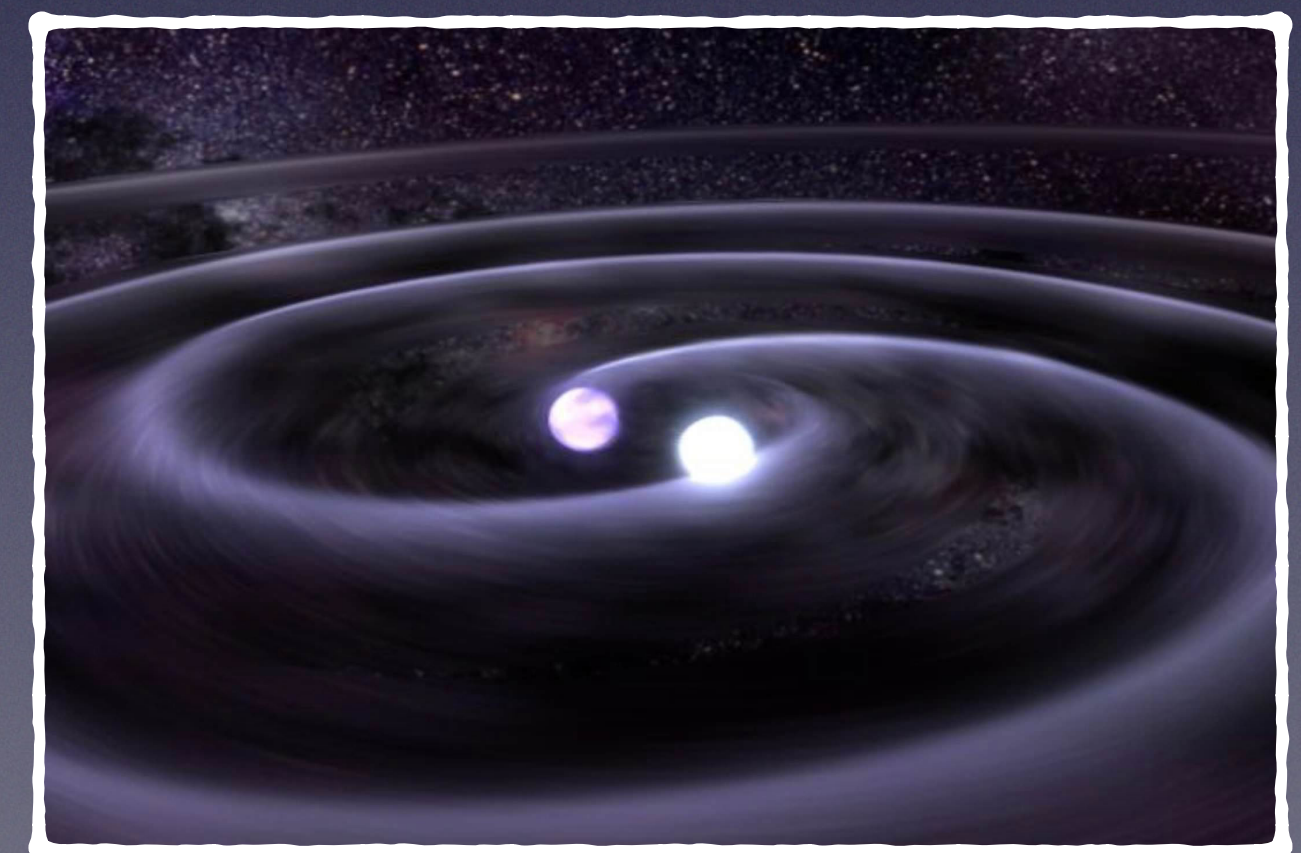
From the Hubble Legacy Archive.
Processing by Judy Schmidt.

$T_{90} < 2s$
(Kouveliotou+93)

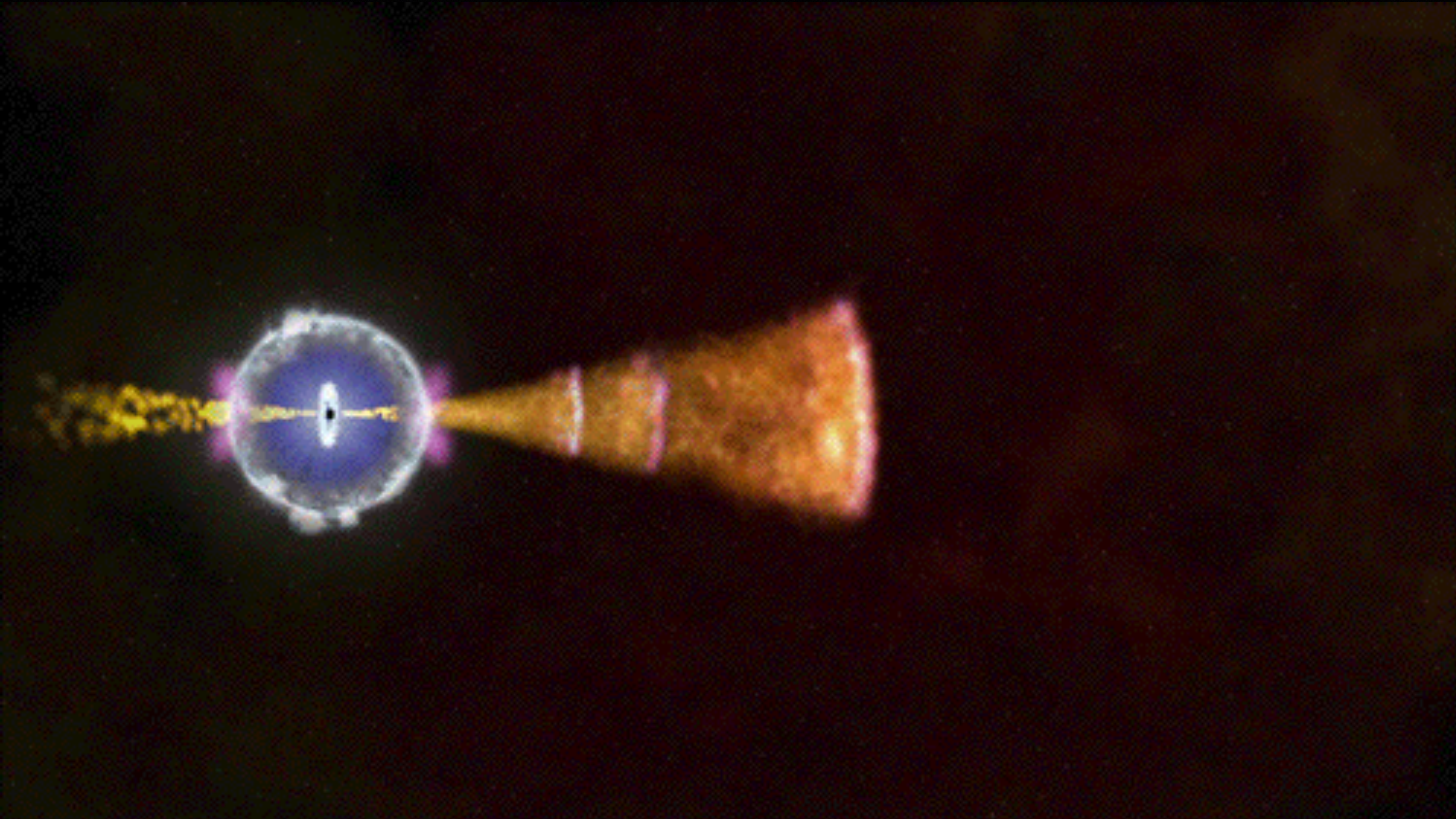
$\langle z \rangle \simeq 0.5$
(Berger13,...)

All morphological types of galaxies
(Berger09, Fong+13, Berger13,...)

[Recently] Associated with KNe
(Tanvir+13,...)



Credits: NASA's Goddard Space Flight Center



GRBs in Radio

Emission mechanism

Forward vs Reverse shocks

Geometry

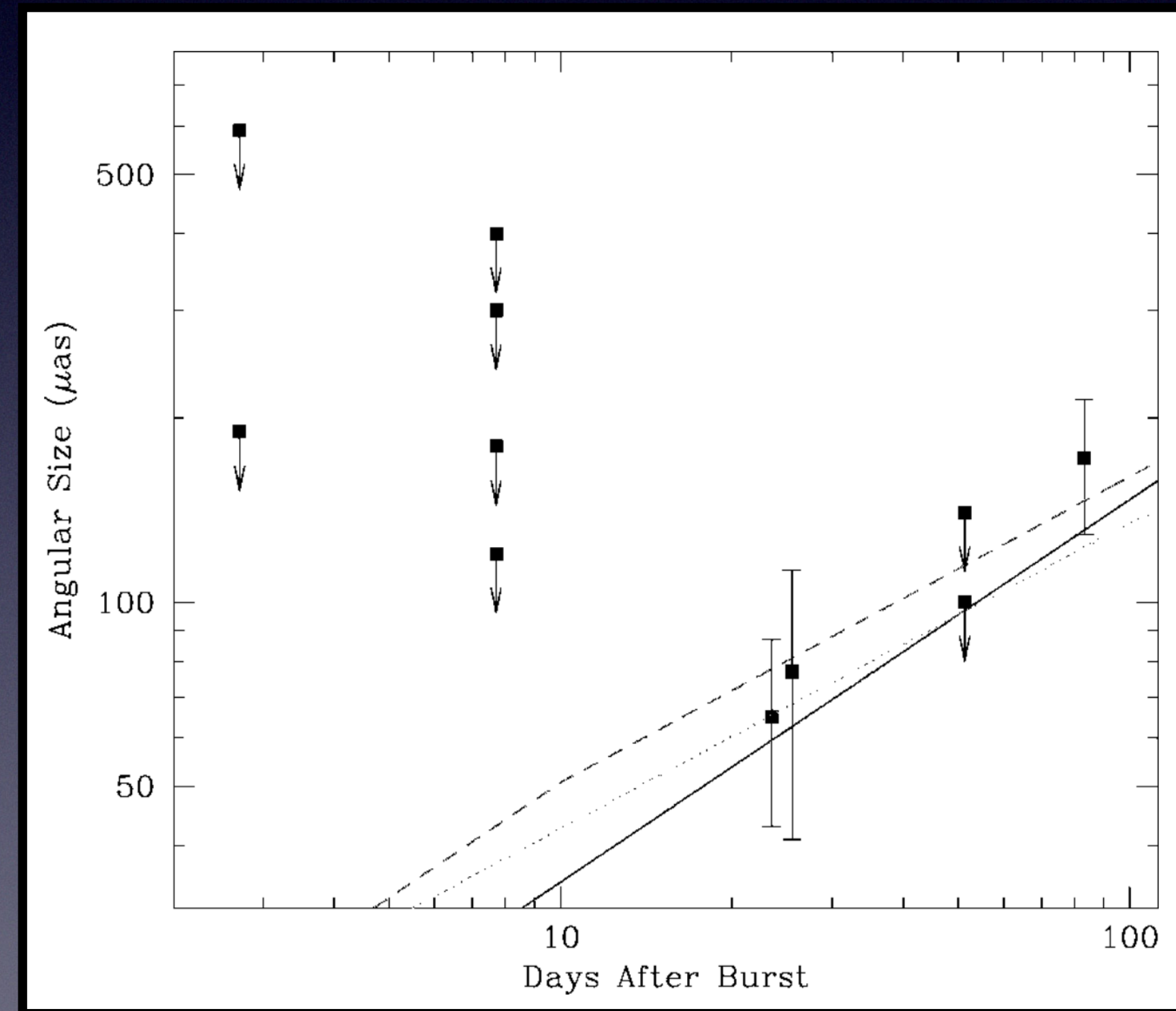
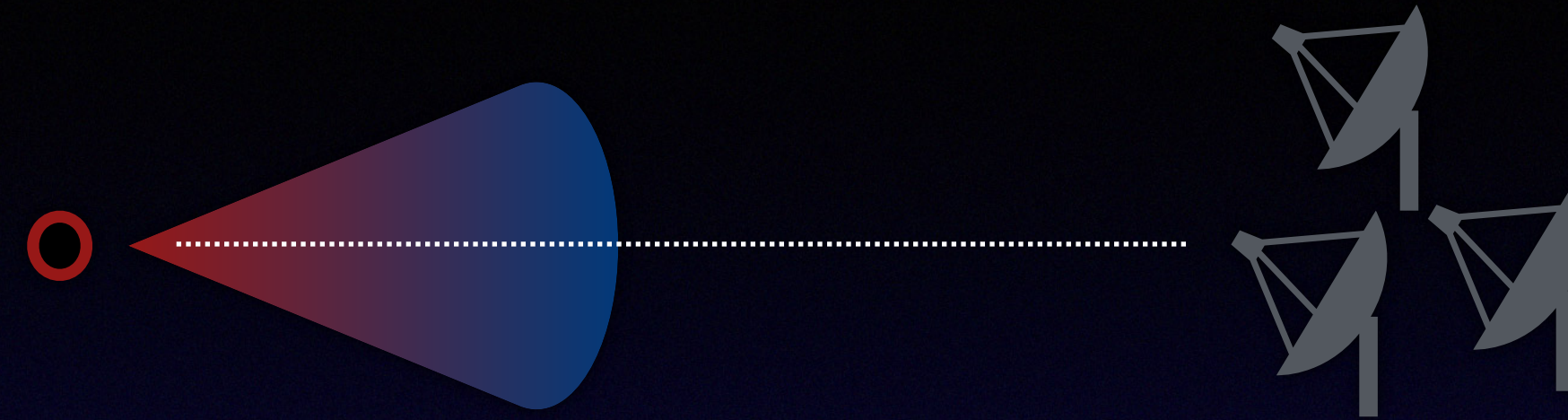
Viewing angle
Collimation angle
Size and structure

Progenitors

Circumburst density profile

See Om's
talk

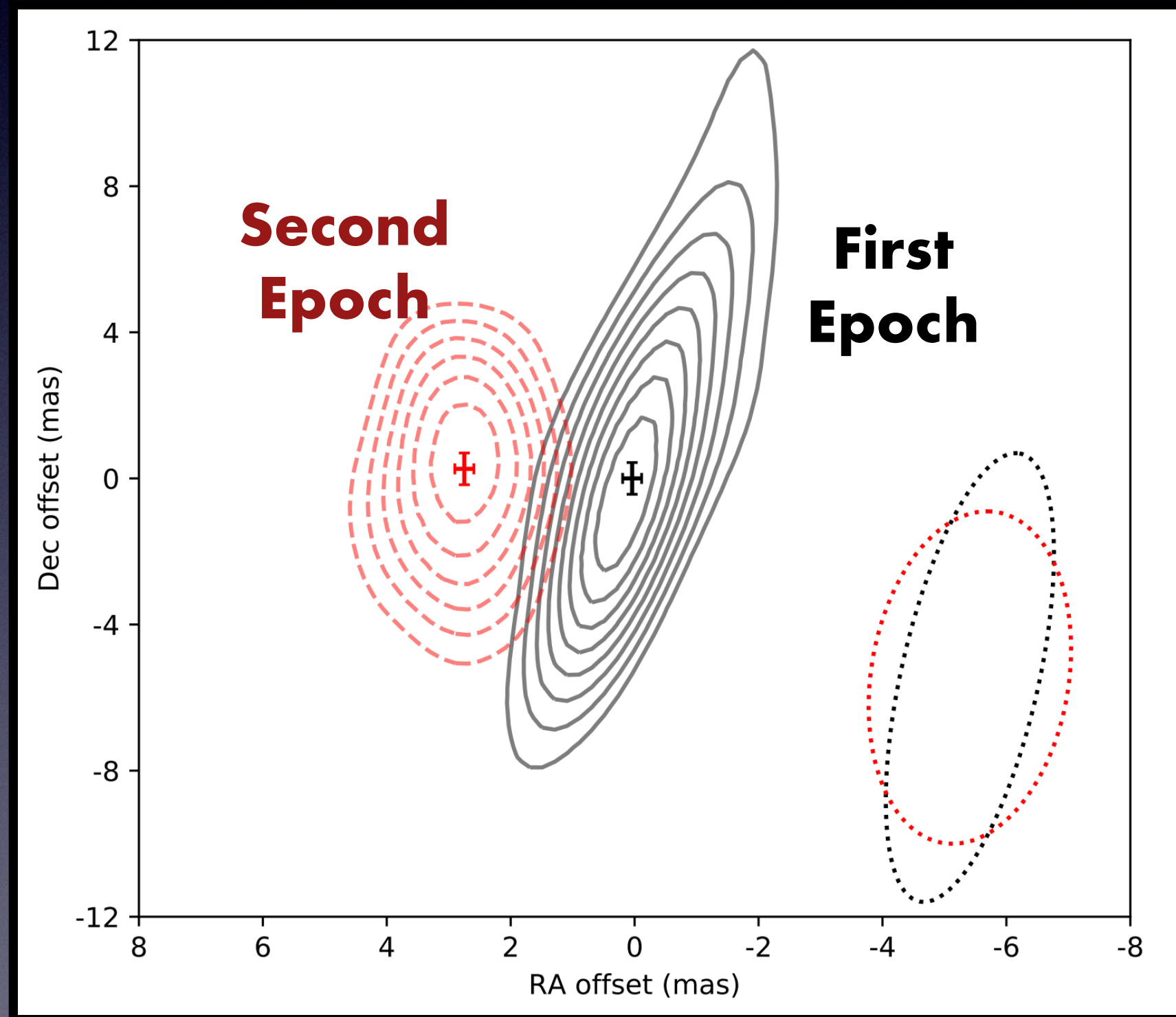
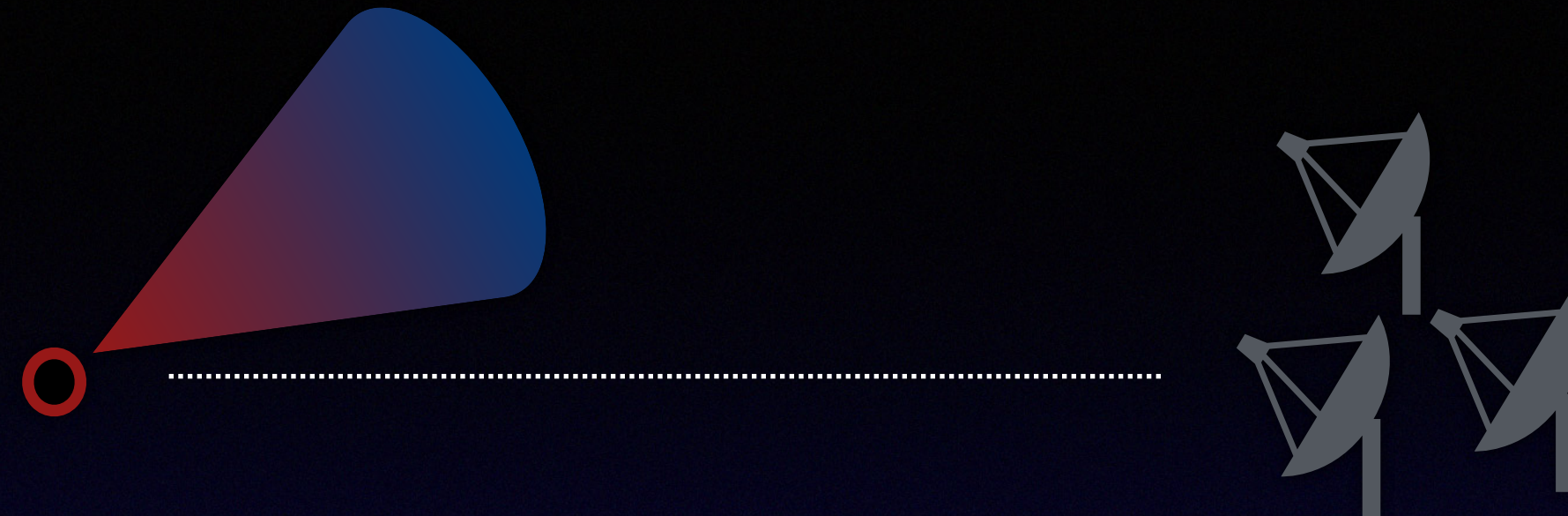
High resolution studies of GRBs



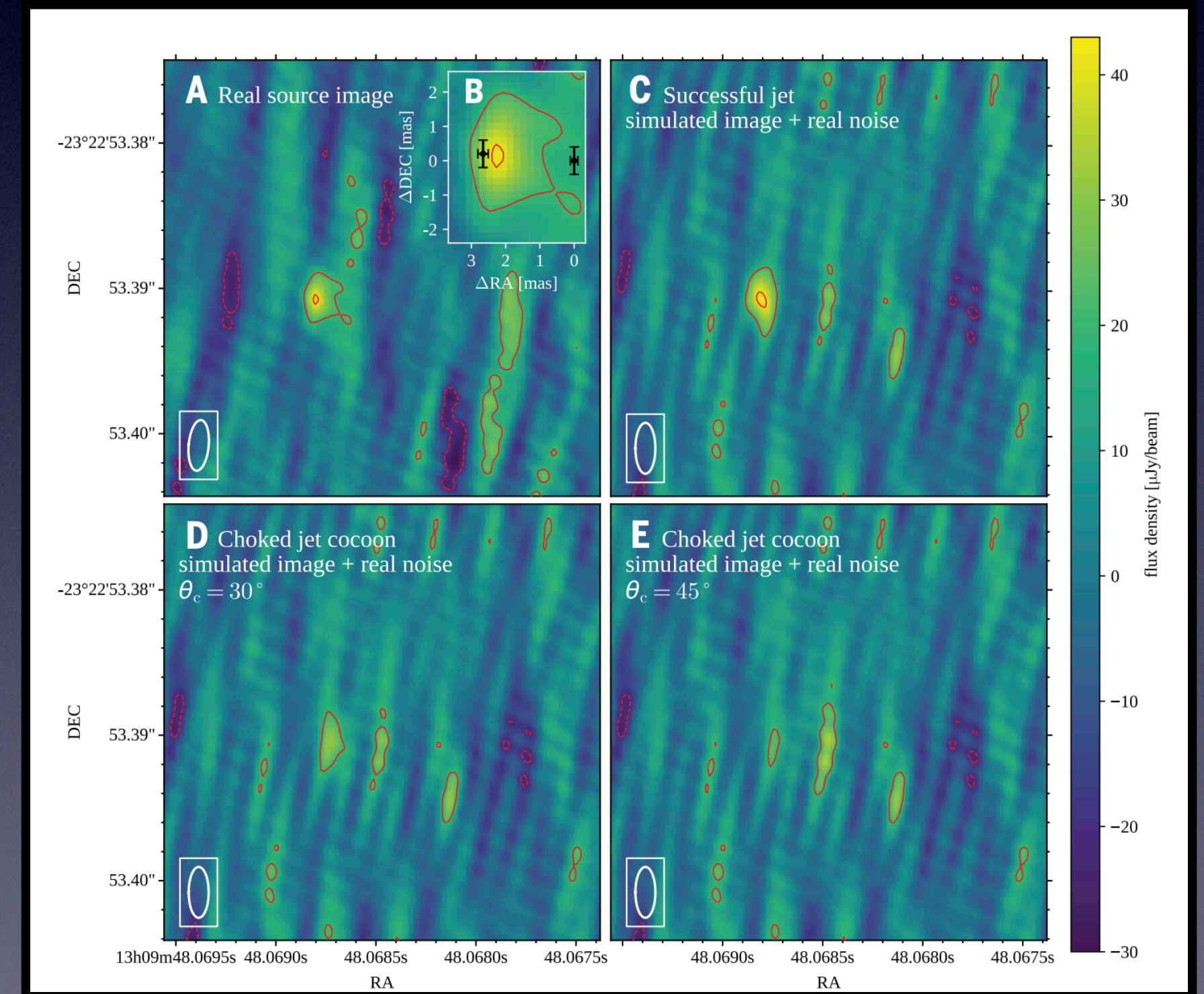
Angular diameter increase: GRB 030329
From *Taylor et al. (2003)*

High resolution studies of GRBs

See Om's talk



Centroid displacement: GRB 170817A
From *Mooley et al. (2018)*

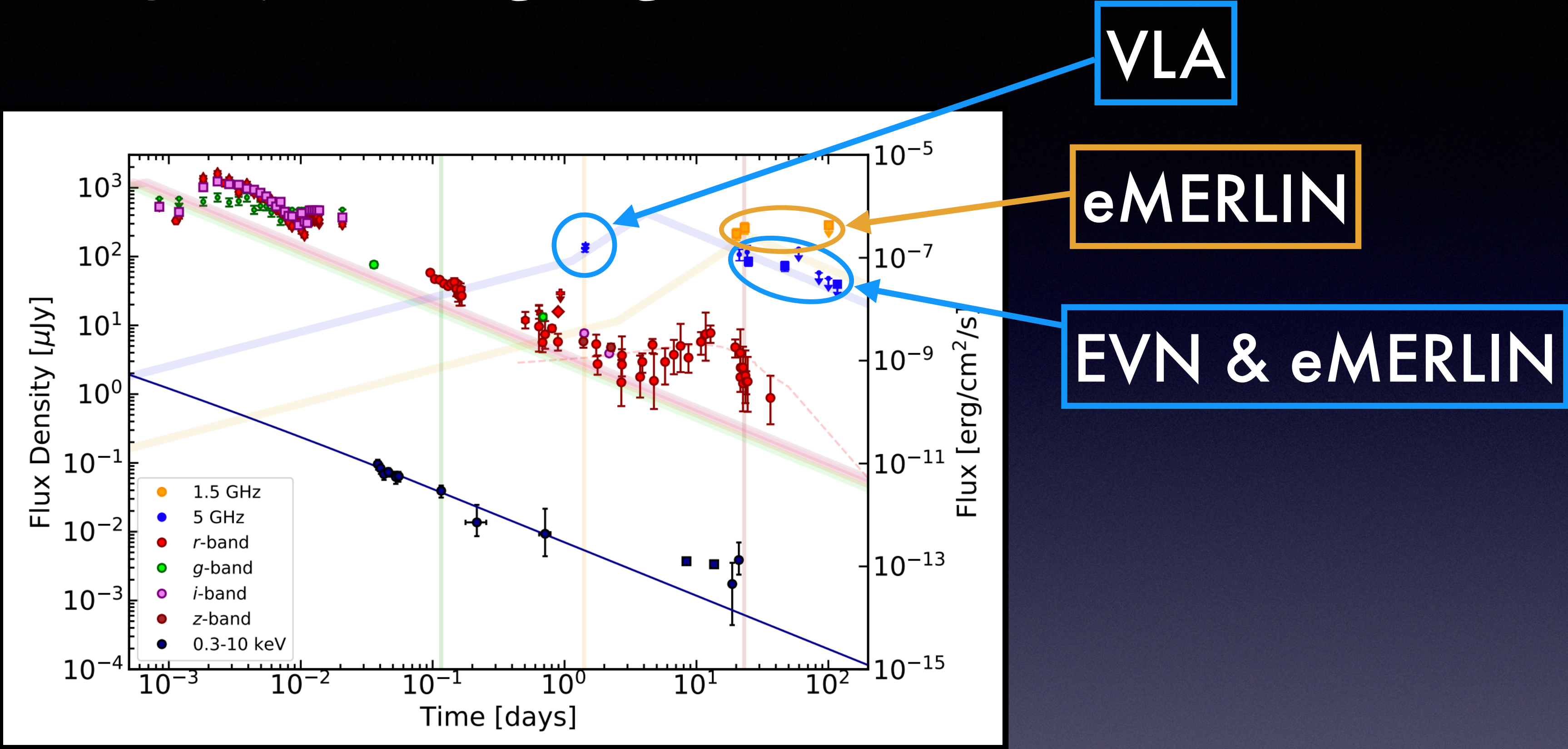


Real and simulated images: GRB 170818A
From *Ghirlanda et al. (2019)*

GRB 201015A

Hint of VHE emission!

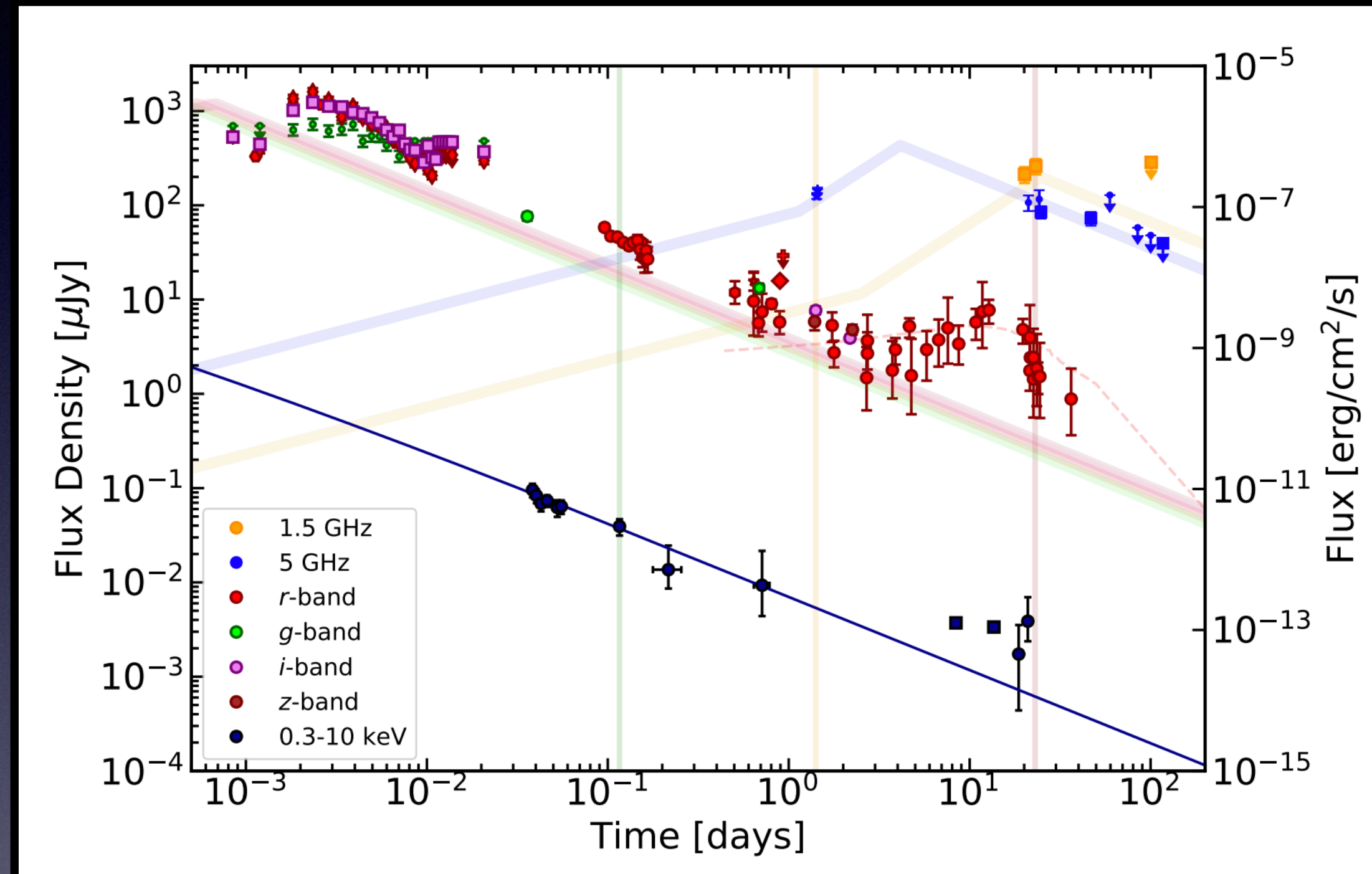
GRB 201015A



Multi-wavelength afterglow light curves of GRB 201015A
From Giarratana et al. (2022)

See also: Suda et al. (2022), Komesh et al. (2023), Ror et al. (2023)

GRB 201015A

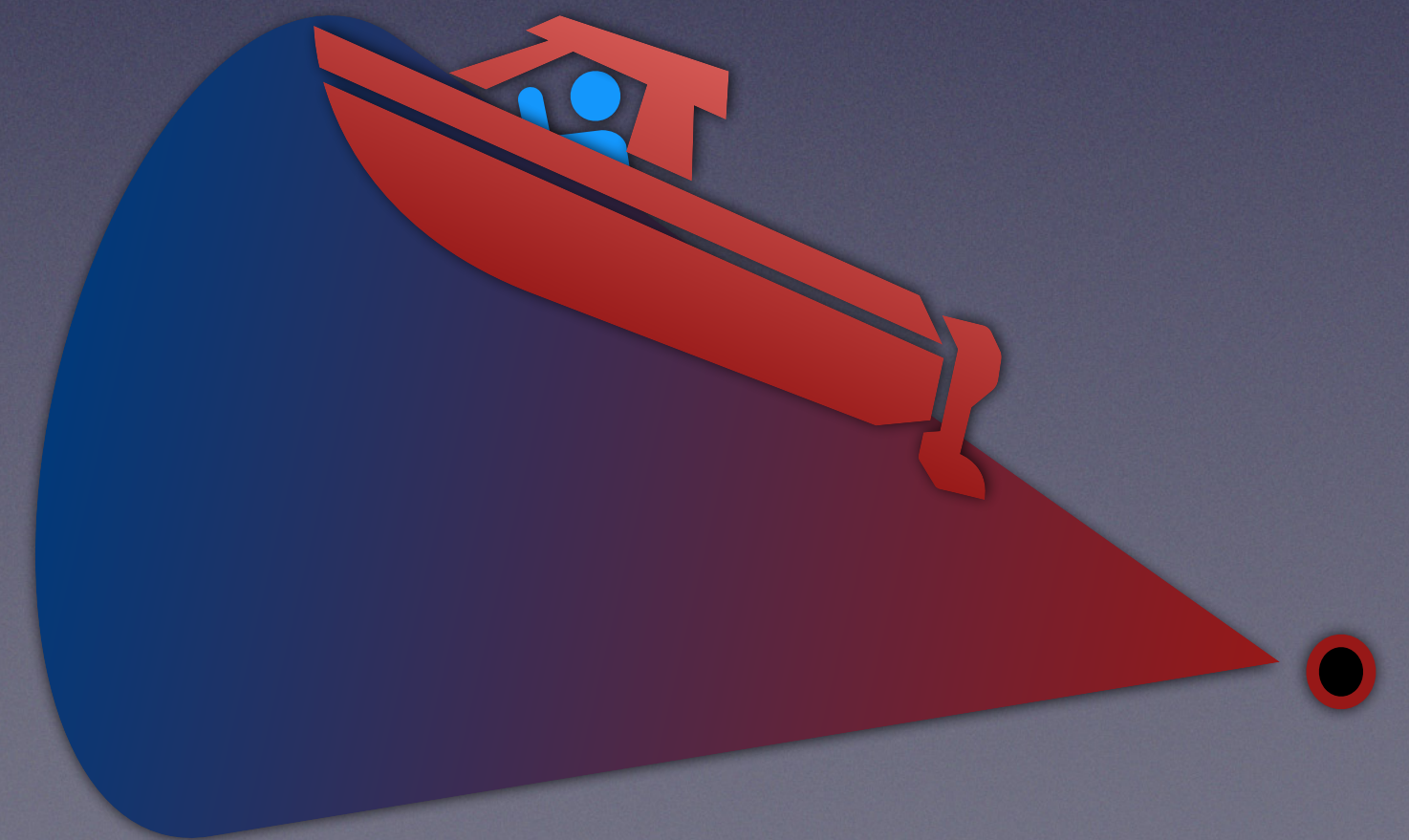


Multi-wavelength afterglow light curves of GRB 201015A
From *Giarratana et al. (2022)*

GRB	z	mas	pc	if z = 0.426
170817A	0.0093	2.44	0.46	0.08
030329A	0.1685	0.17	0.5	0.09

Displacement	Size
Gamma(Dec) < 61	< 5 pc at 25 d
Gamma(RA) < 40	< 16 pc at 47 d

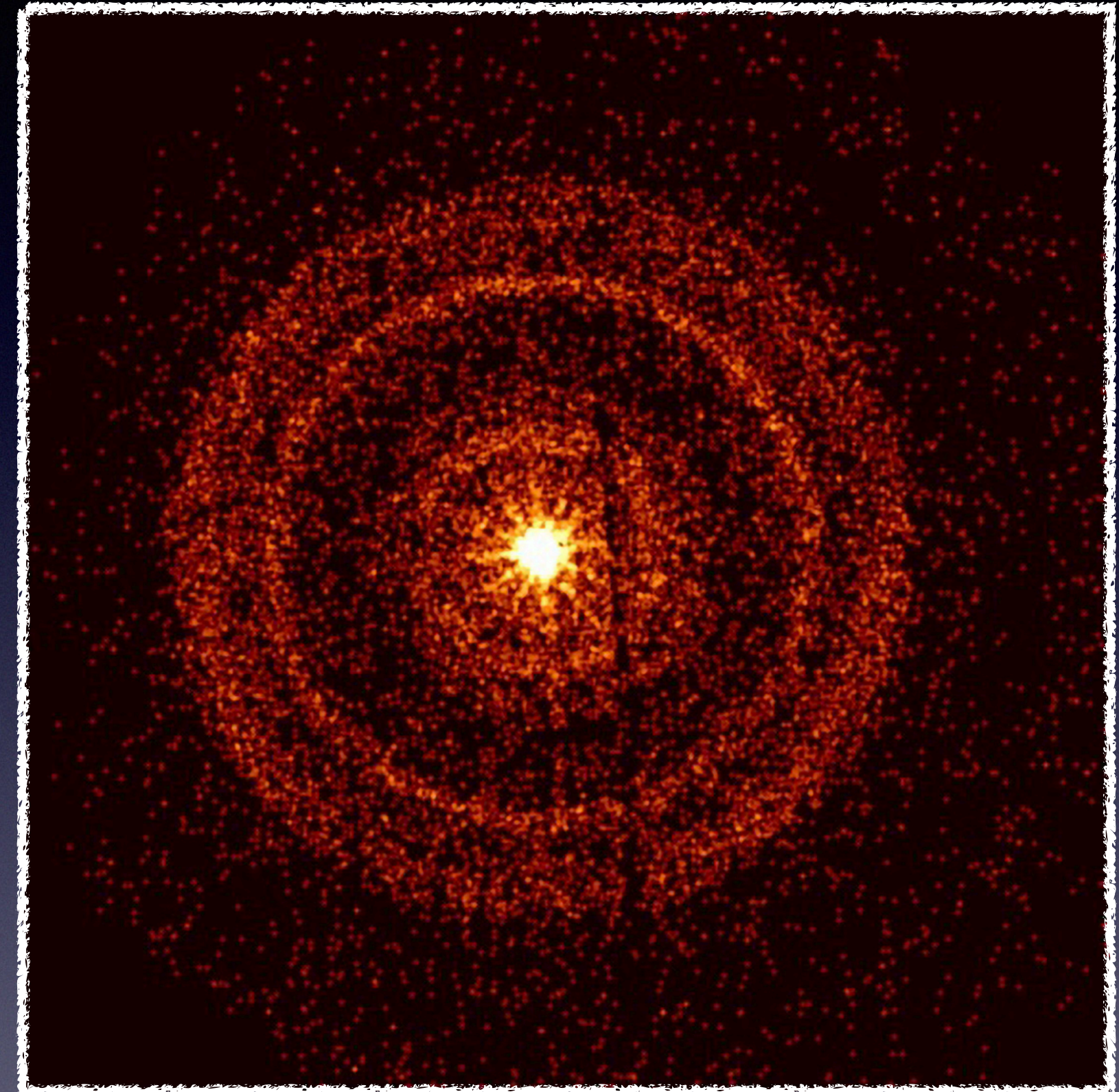
GRB 221009A: the **B**rightest **O**f **A**ll **T**ime



GRB 221009A

TeV
emission!

- $T_{90} = 327 \text{ s}$ (10 - 1000 keV; GCN 32642)
- $E_{iso} \simeq 3 \times 10^{54} \text{ erg}$ (GCN 32668)
- $z = 0.151$ (GCN 32648, 32686,...)



Credit: NASA/Swift/A.
Beardmore (University of Leicester)

A Significant Sudden Ionospheric Disturbance associated with Gamma-Ray Burst GRB 221009A

LAURA A. HAYES¹ AND PETER T. GALLAGHER²

¹European Space Agency (ESA), European Space Research and Technology Centre (ESTEC),
Keplerlaan 1, 2201 AZ Noordwijk, The Netherlands

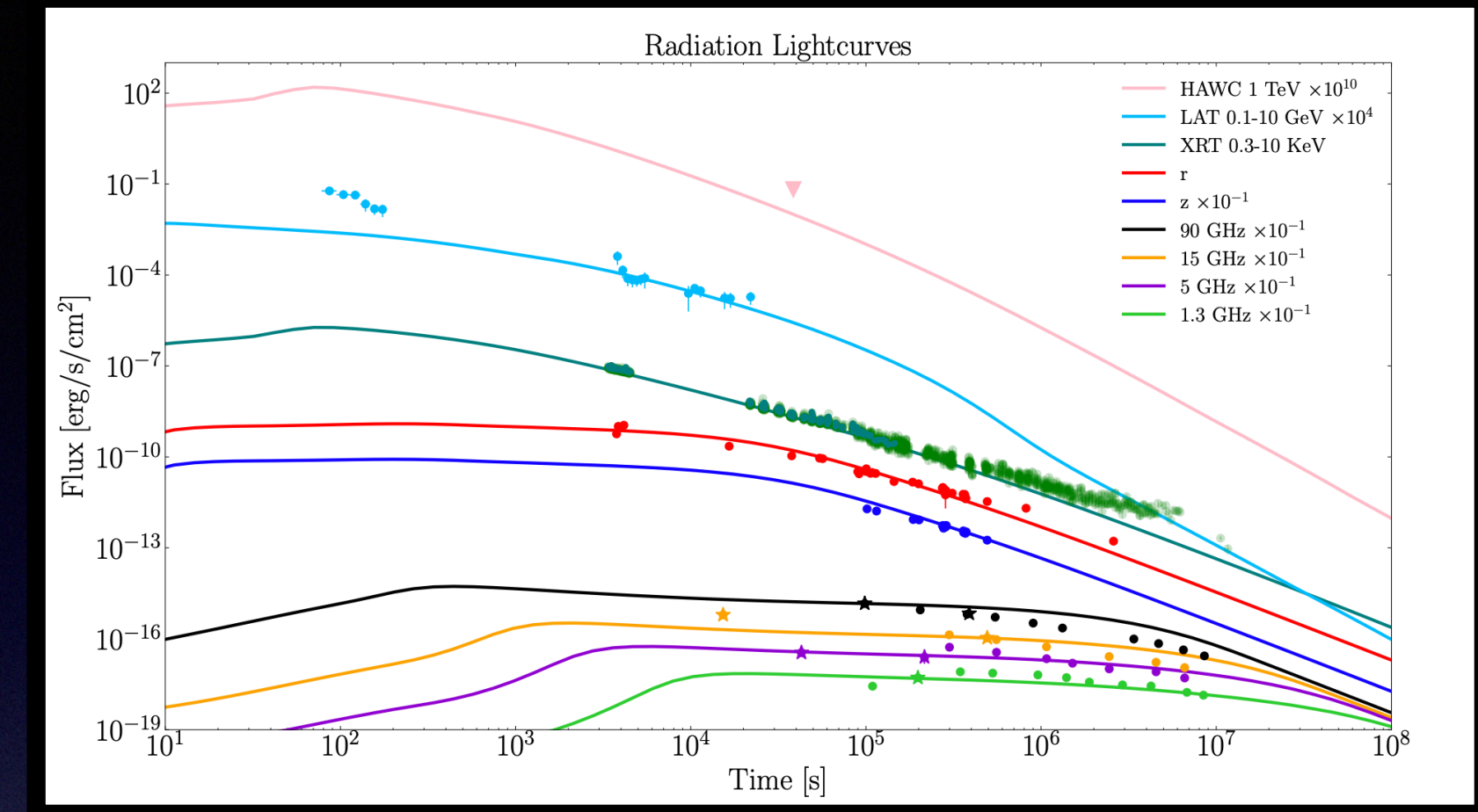
²Astronomy & Astrophysics Section, DIAS Dunsink Observatory, Dublin Institute for Advanced Studies, Dublin, Ireland

ABSTRACT

We report a significant sudden ionospheric disturbance (SID) in the D-region of Earth's ionosphere (~60–100 km), which was associated with the massive γ -ray burst GRB 221009A on 2022 October 9. We identified the SID over northern Europe—a result of ionisation by X- and γ -ray emission from the GRB—using very low frequency (VLF) radio waves as a probe of the D-region. These observations demonstrate that an extra-galactic GRB ($z \sim 0.151$) can have a significant impact on the terrestrial atmosphere and illustrates that the Earth's ionosphere can be used as a giant X- and γ -ray detector. Indeed, these observations may provide an insight into the impacts of GRBs on the ionospheres of planets in our Solar System and beyond.

Afterglow Models

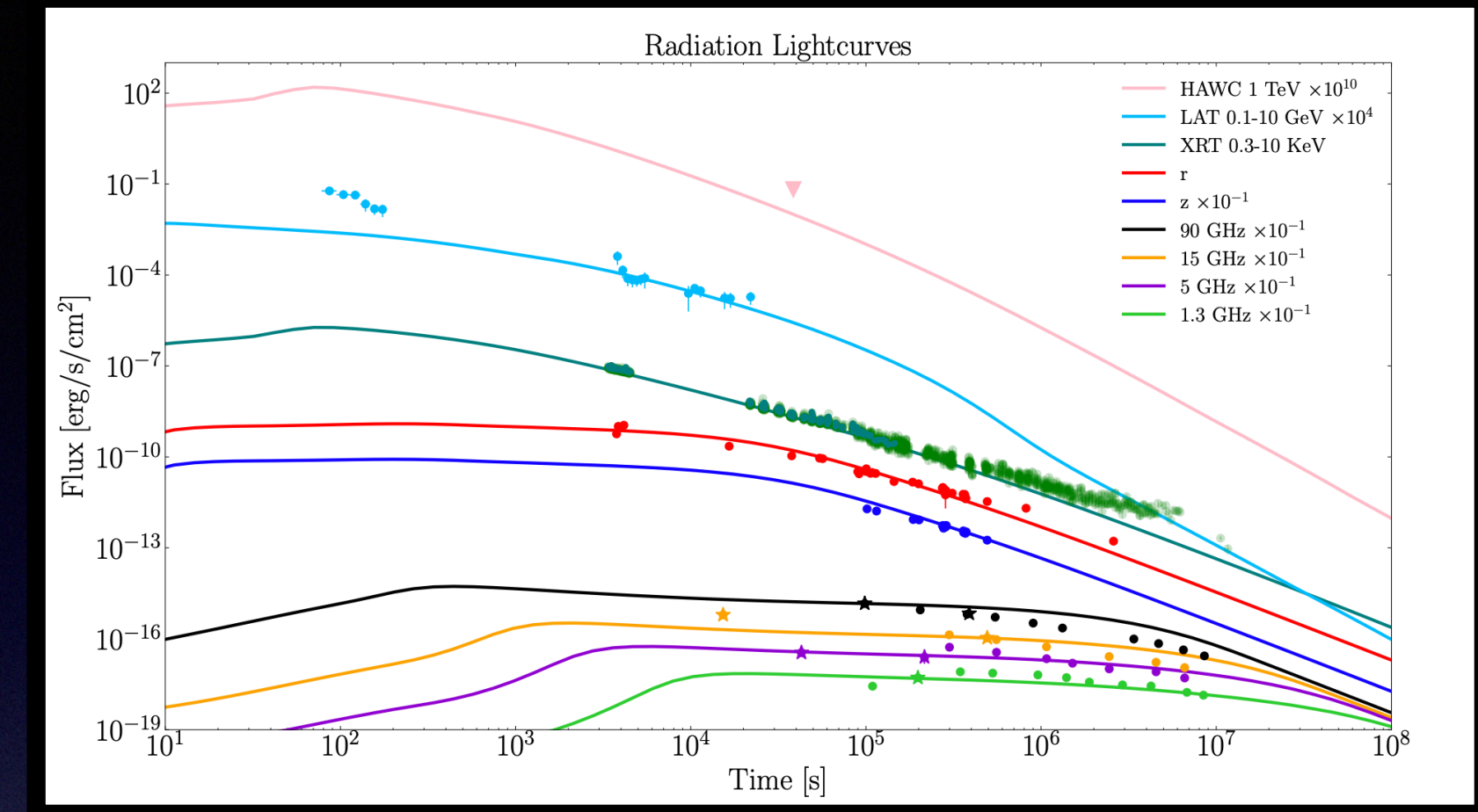
- (1) *Ren et al. (2023)*: top-hat jet in a wind-like environment
- (2) *Sato et al. (2023)*: two-component jet in a uniform environment
- (3) *Laskar et al. (2023)*: FS from a jet in a low-density wind-like environment
- (4) *O'Connor et al. (2023)*: structured jet in a medium with $k < 4/3$



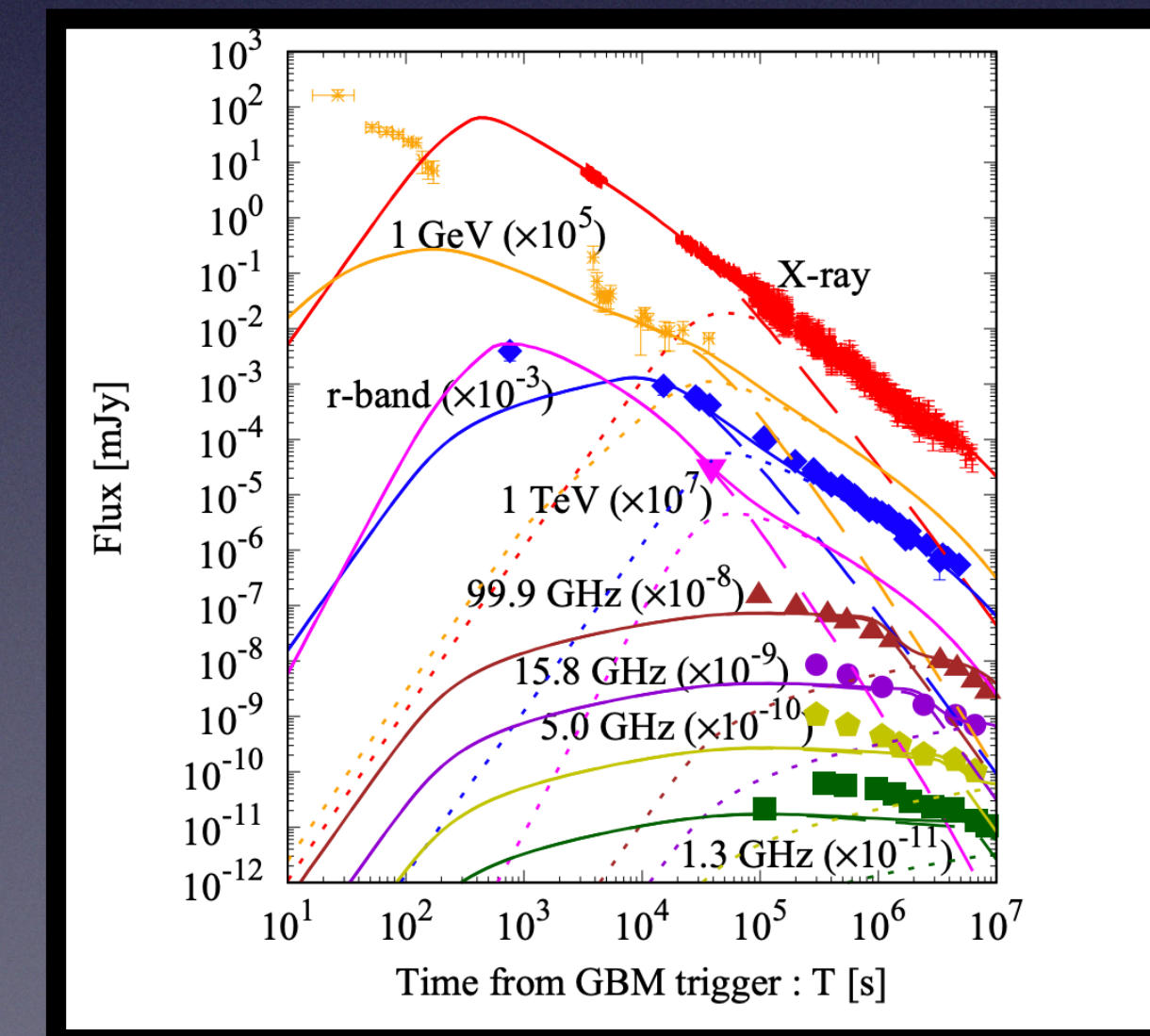
Top-hat jet model
From *Ren et al. (2023)*

Afterglow Models

- (1) *Ren et al. (2023)*: top-hat jet in a wind-like environment
- (2) *Sato et al. (2023)*: two-component jet in a uniform environment
- (3) *Laskar et al. (2023)*: FS from a jet in a low-density wind-like environment
- (4) *O'Connor et al. (2023)*: structured jet in a medium with $k < 4/3$



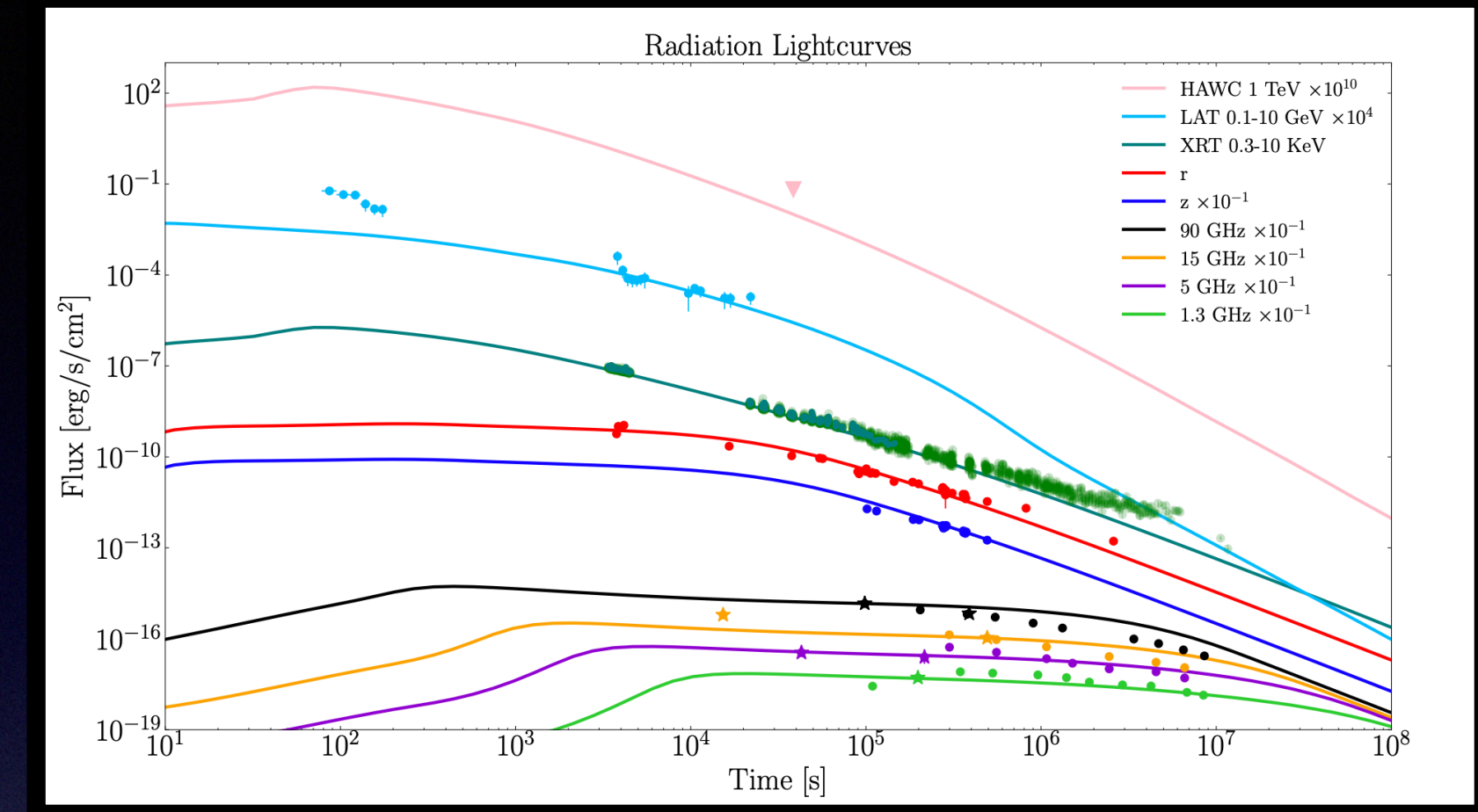
Top-hat jet model
From *Ren et al. (2023)*



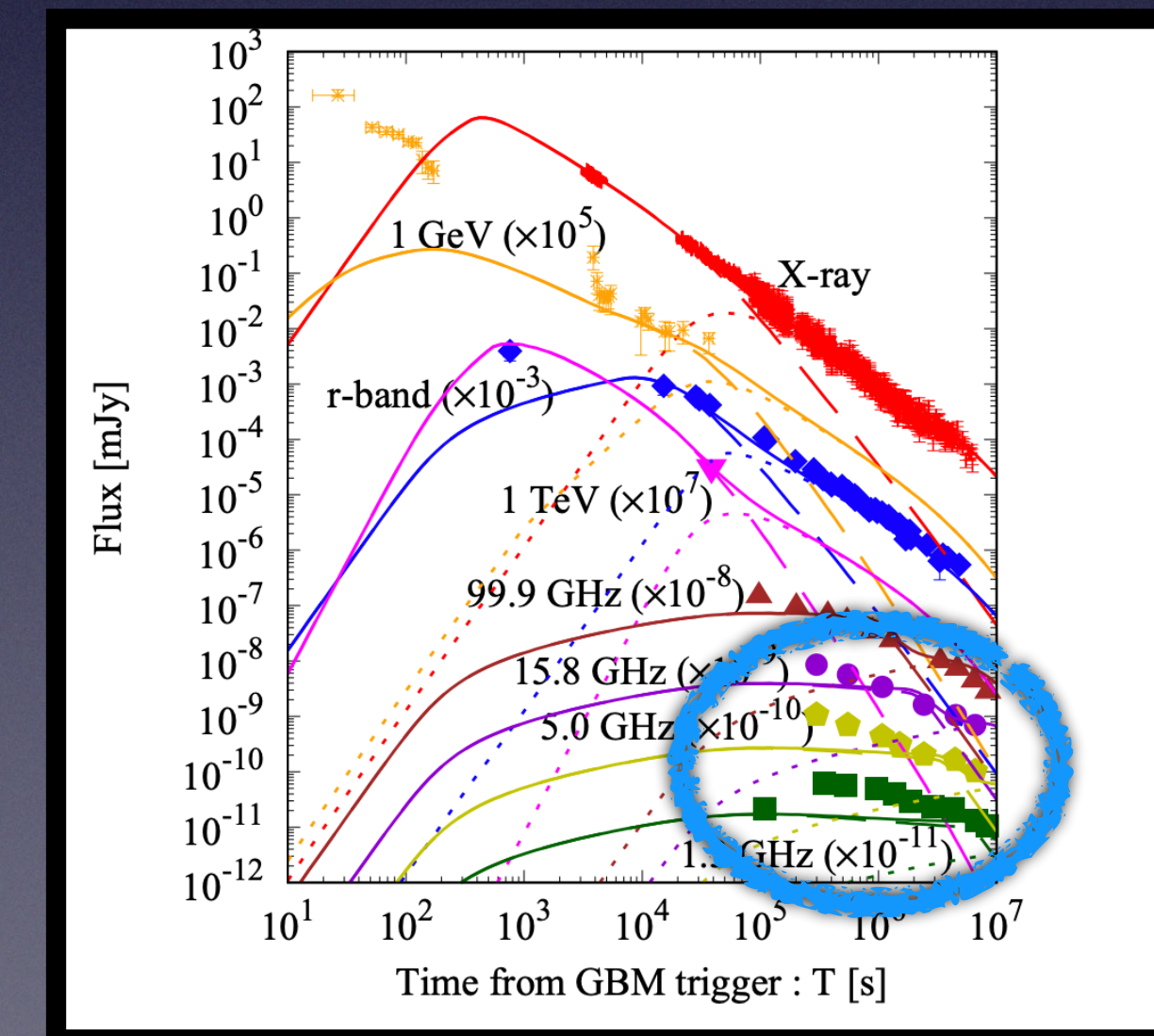
Two-component jet model
From *Sato et al. (2023)*

Afterglow Models

- (1) *Ren et al. (2023)*: top-hat jet in a wind-like environment
- (2) *Sato et al. (2023)*: two-component jet in a uniform environment
- (3) *Laskar et al. (2023)*: FS from a jet in a low-density wind-like environment
- (4) *O'Connor et al. (2023)*: structured jet in a medium with $k < 4/3$



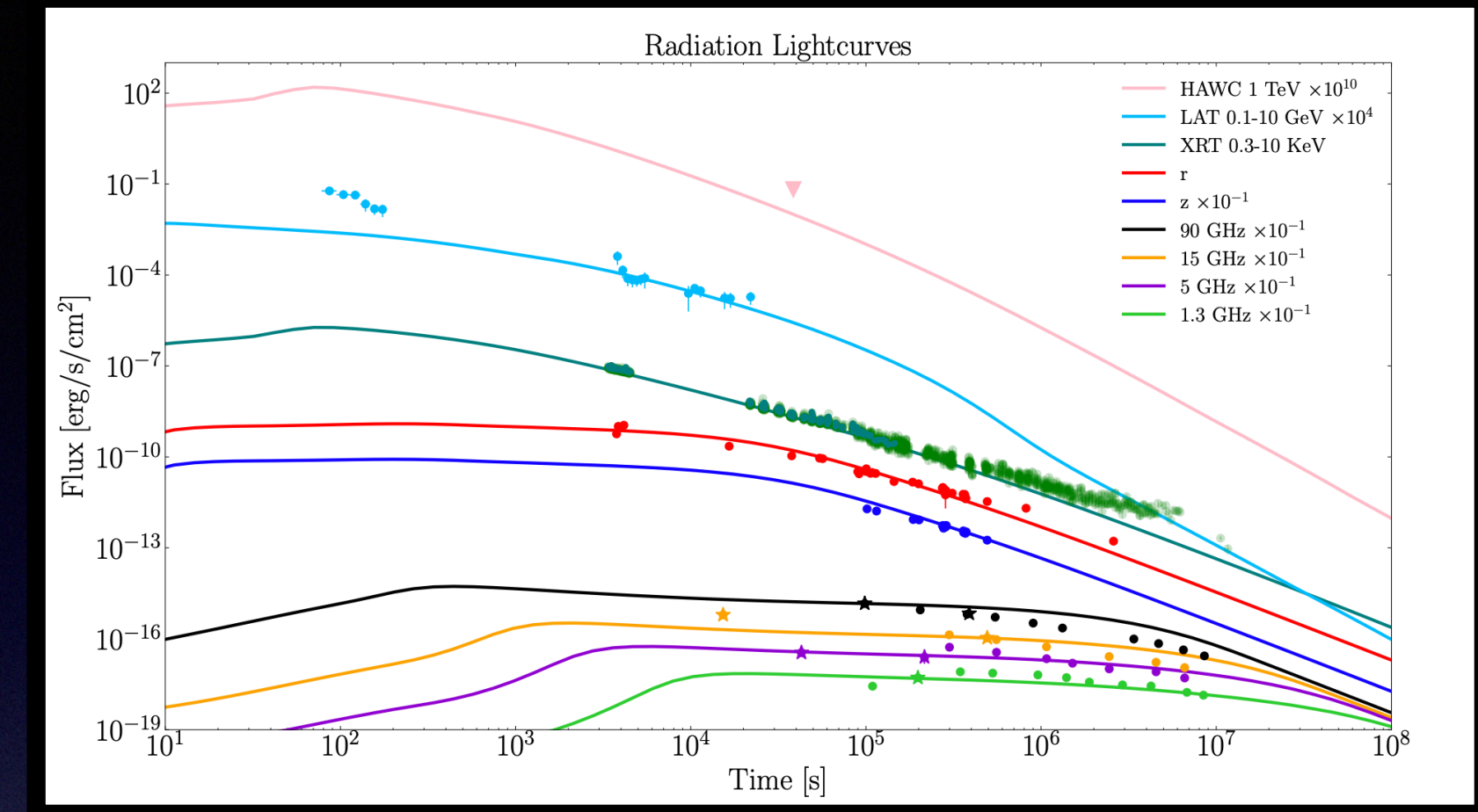
Top-hat jet model
From *Ren et al. (2023)*



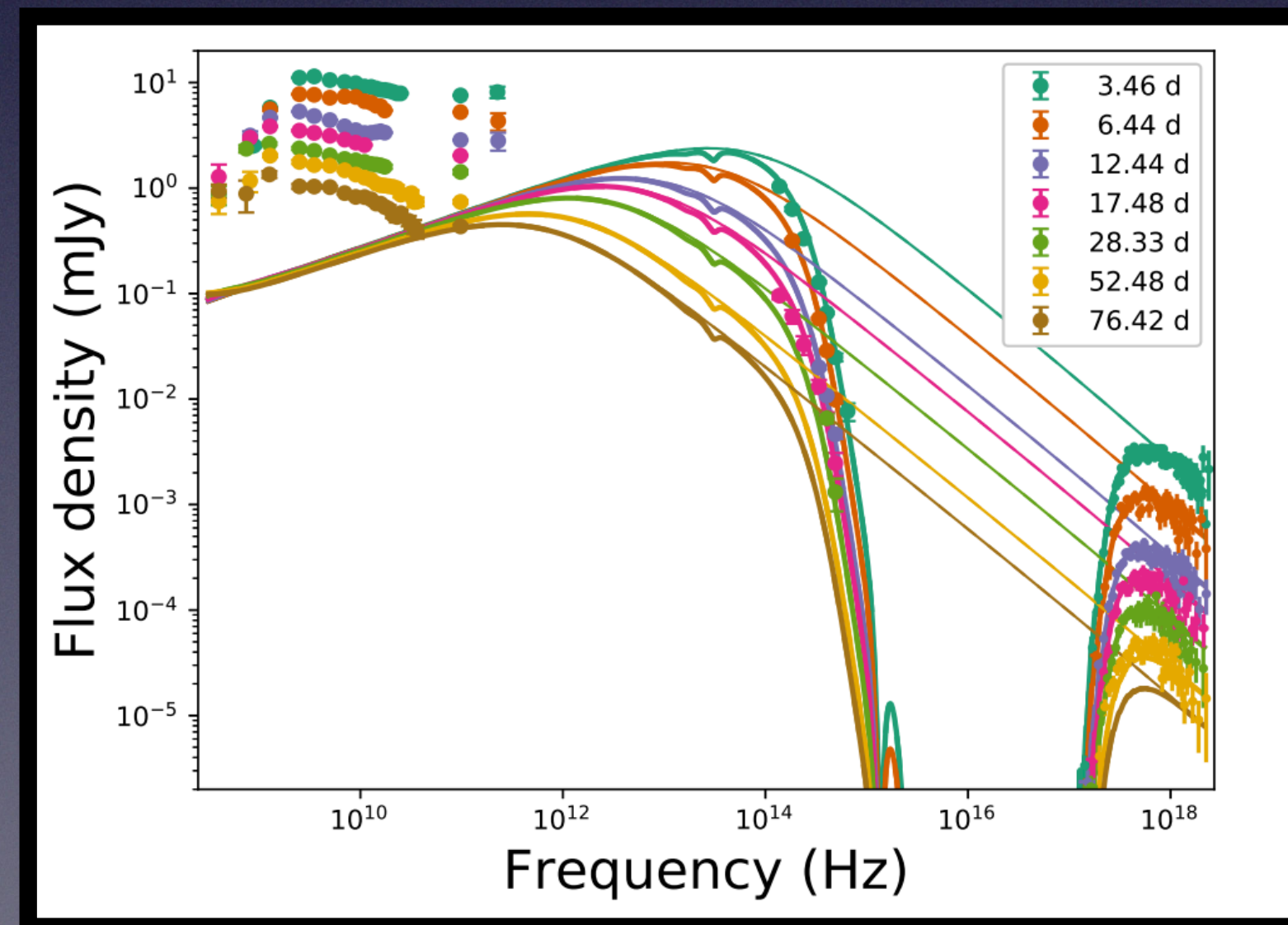
Two-component jet model
From *Sato et al. (2023)*

Afterglow Models

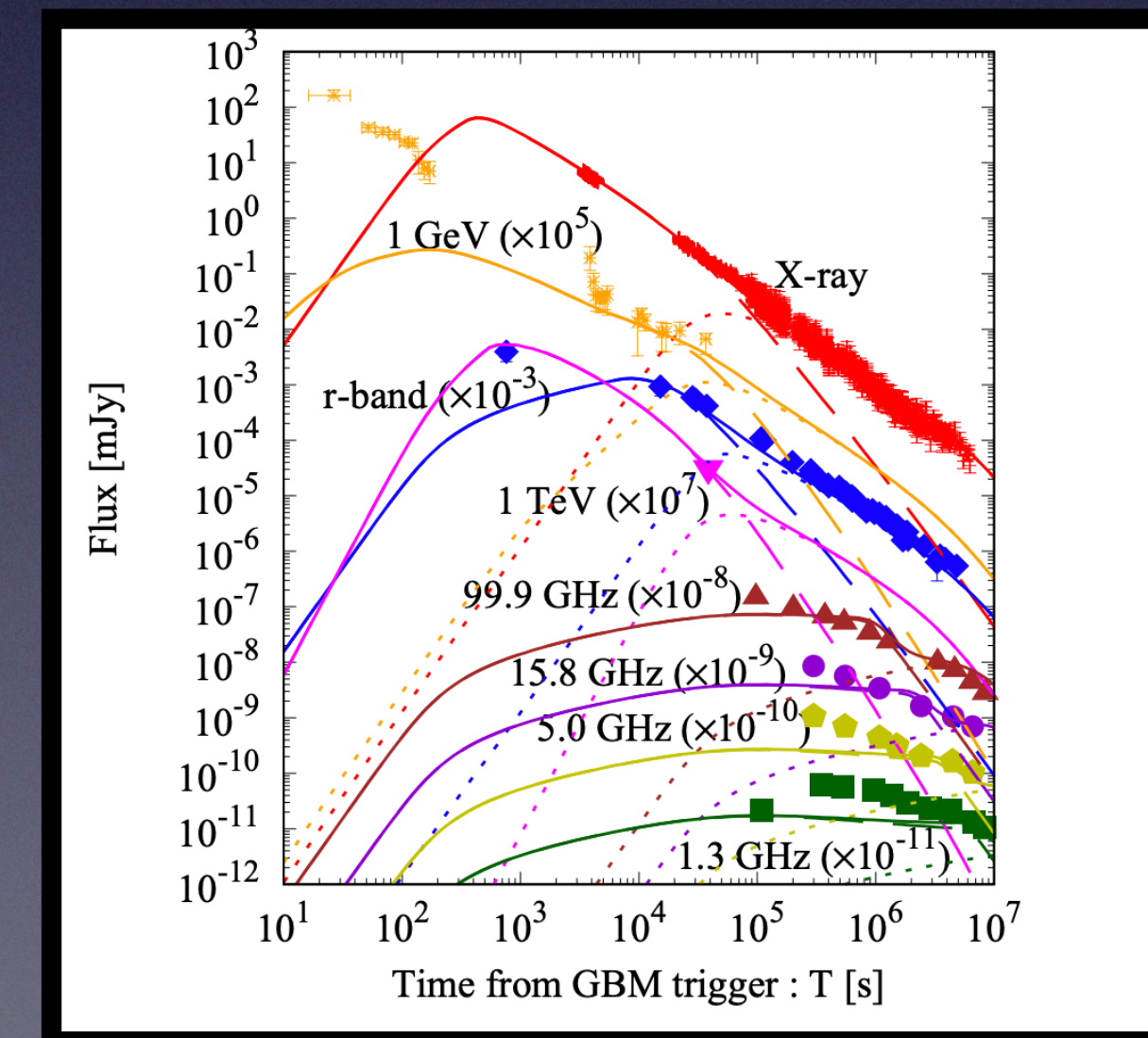
- (1) *Ren et al. (2023)*: top-hat jet in a wind-like environment
- (2) *Sato et al. (2023)*: two-component jet in a uniform environment
- (3) *Laskar et al. (2023)*: FS from a jet in a low-density wind-like environment
- (4) *O'Connor et al. (2023)*: structured jet in a medium with $k < 4/3$



Top-hat jet model
From *Ren et al. (2023)*



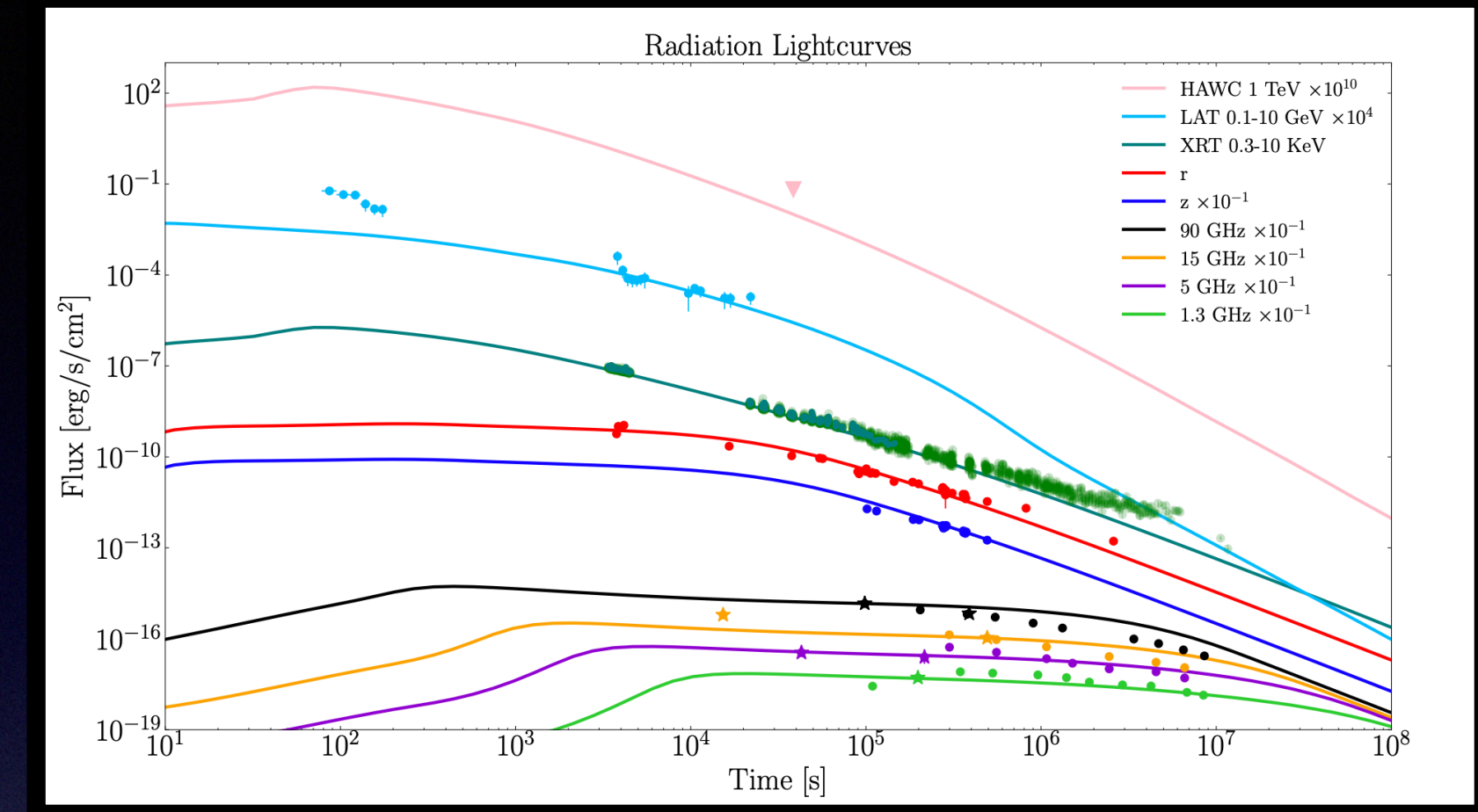
Single FS model
From *Laskar et al. (2023)*



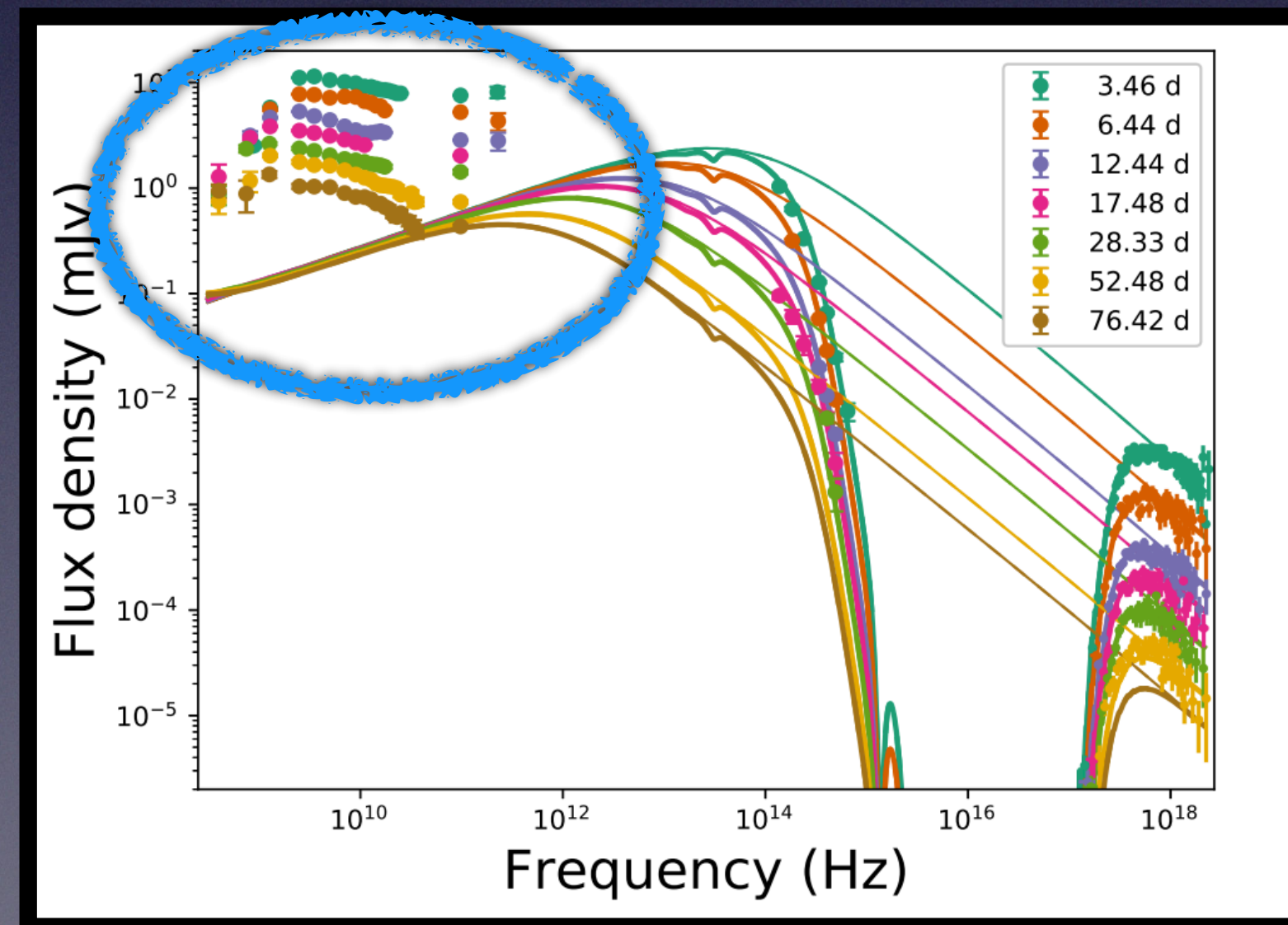
Two-component jet model
From *Sato et al. (2023)*

Afterglow Models

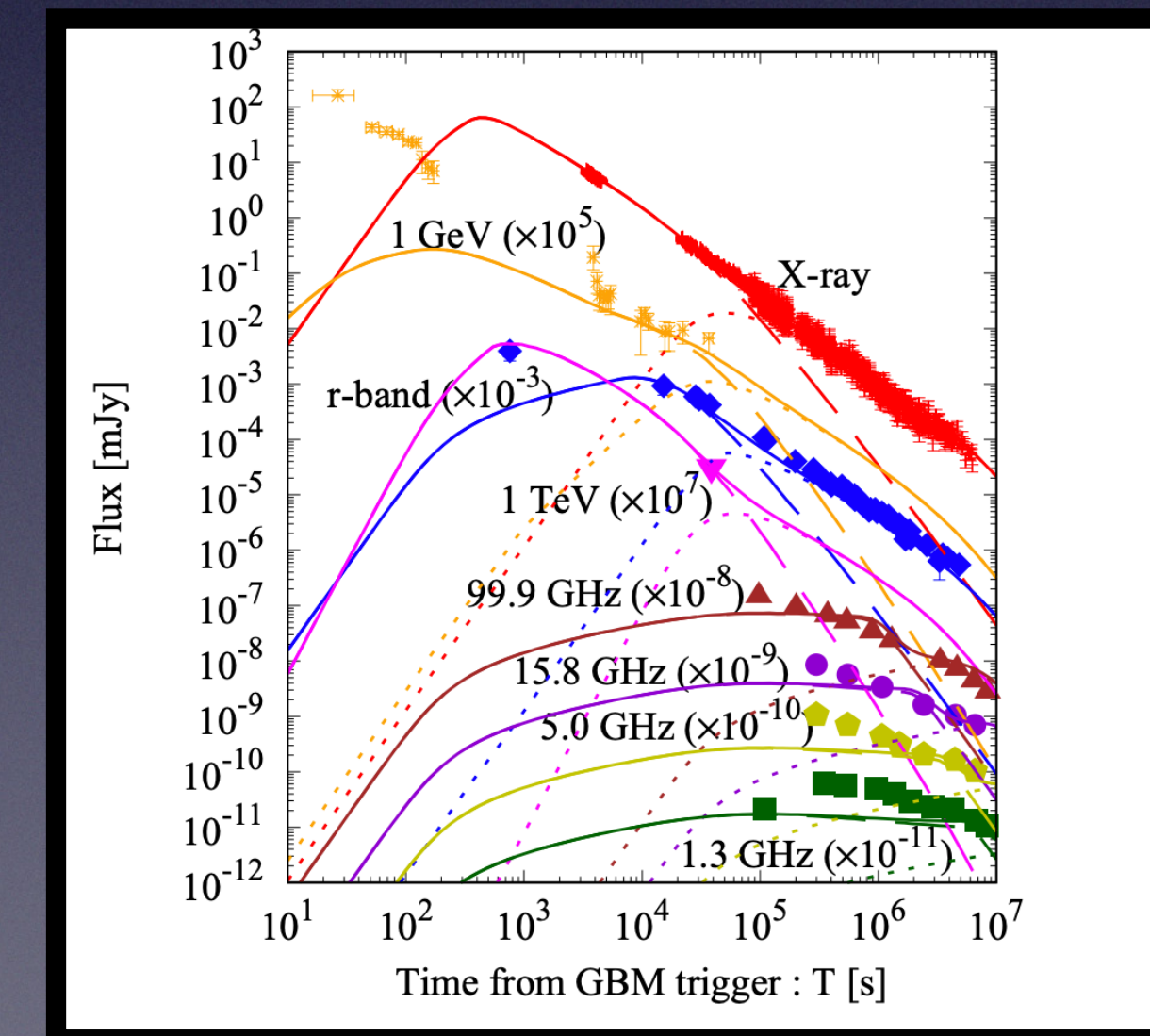
- (1) *Ren et al. (2023)*: top-hat jet in a wind-like environment
- (2) *Sato et al. (2023)*: two-component jet in a uniform environment
- (3) *Laskar et al. (2023)*: FS from a jet in a low-density wind-like environment
- (4) *O'Connor et al. (2023)*: structured jet in a medium with $k < 4/3$



Top-hat jet model
From *Ren et al. (2023)*



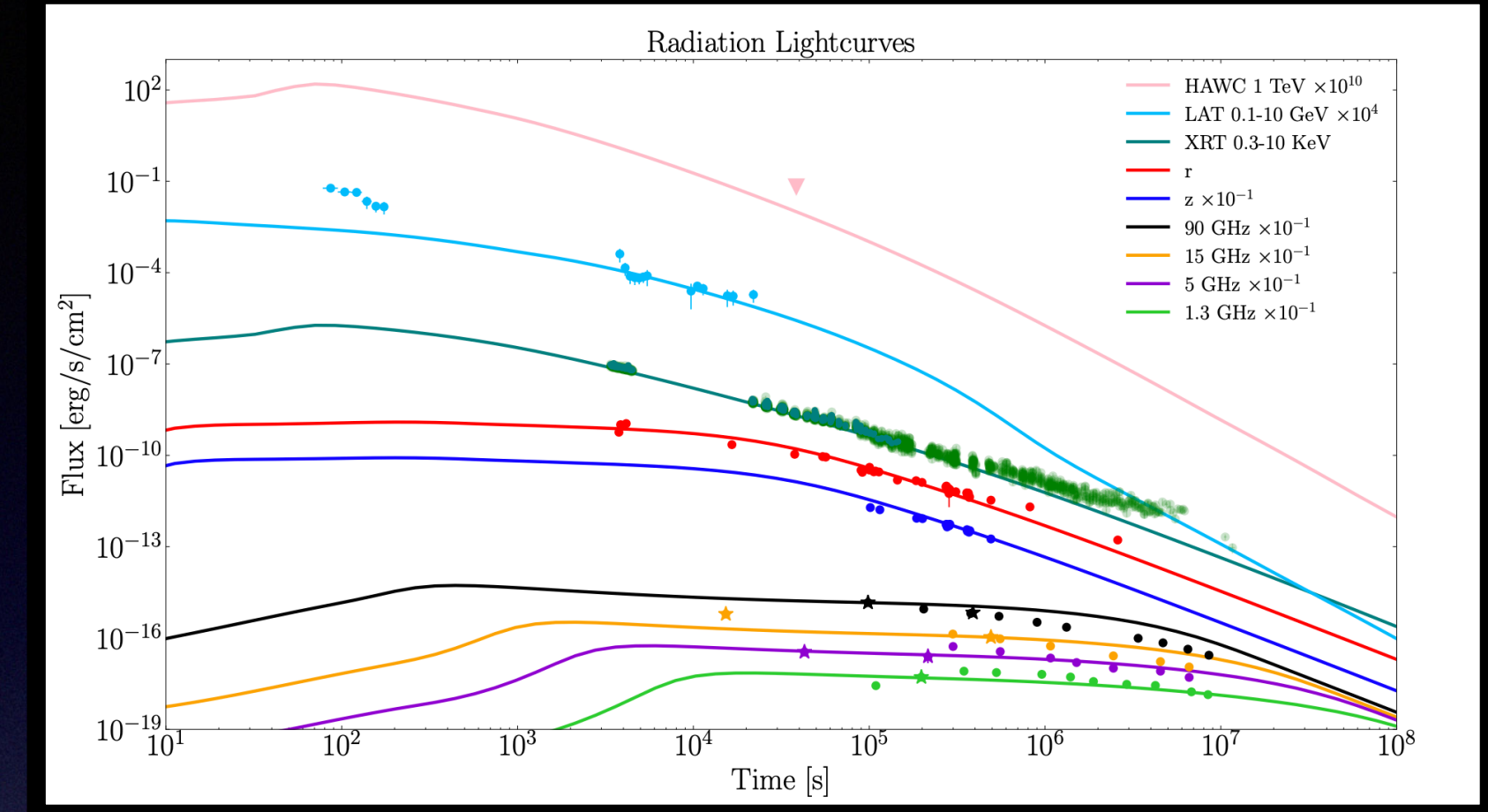
Single FS model
From *Laskar et al. (2023)*



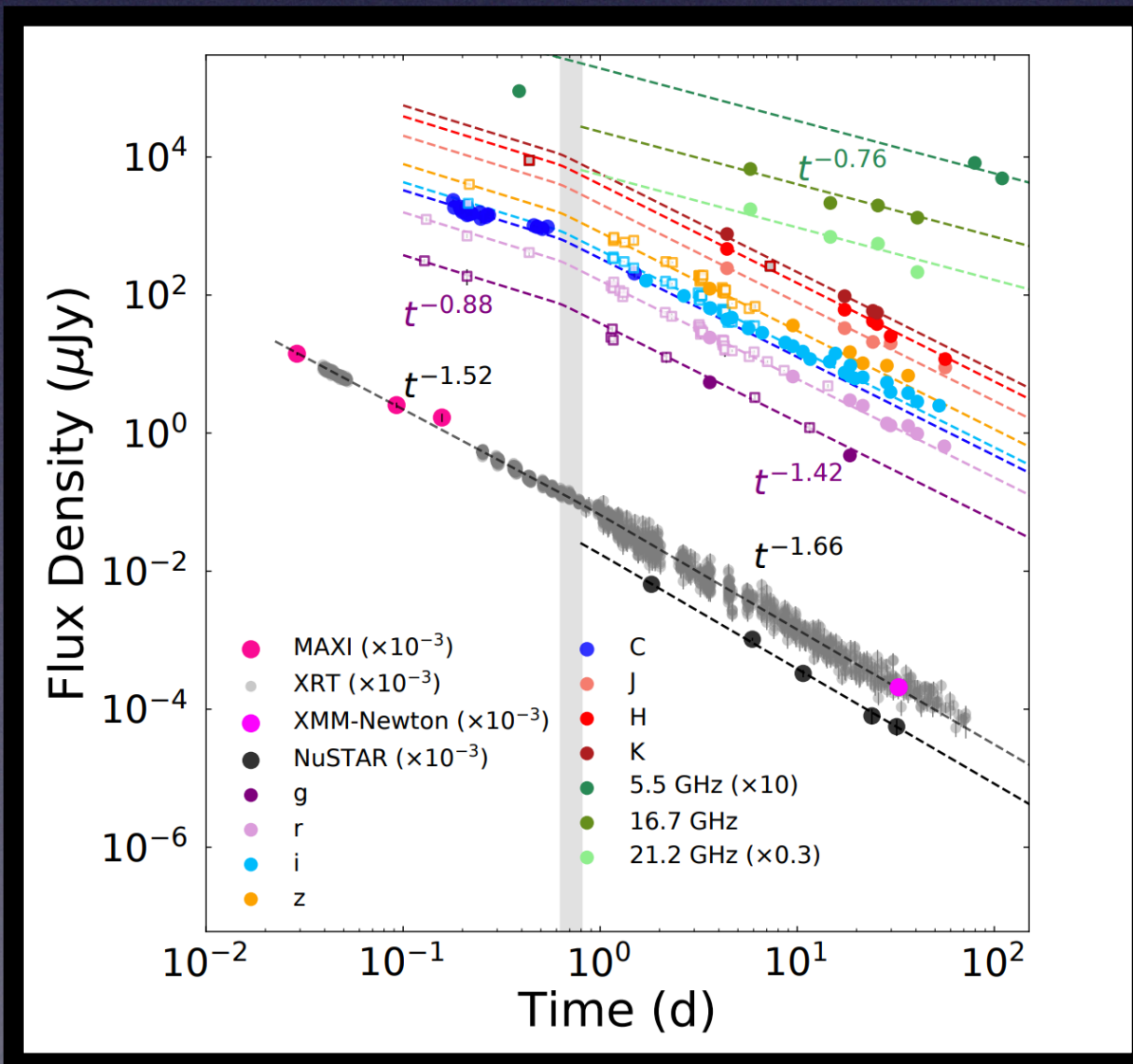
Two-component jet model
From *Sato et al. (2023)*

Afterglow Models

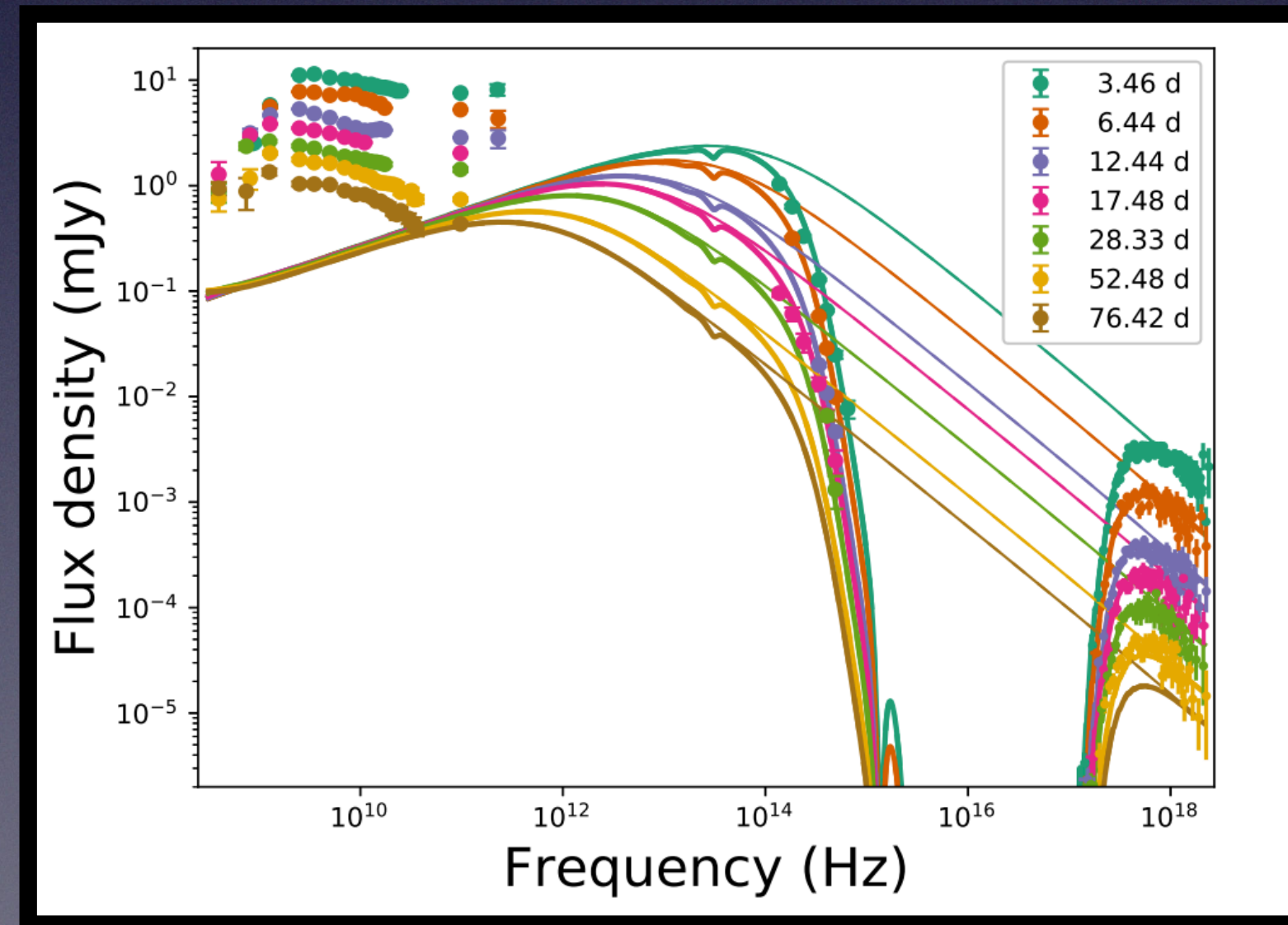
- (1) *Ren et al. (2023)*: top-hat jet in a wind-like environment
- (2) *Sato et al. (2023)*: two-component jet in a uniform environment
- (3) *Laskar et al. (2023)*: FS from a jet in a low-density wind-like environment
- (4) *O'Connor et al. (2023)*: structured jet in a medium with $k < 4/3$



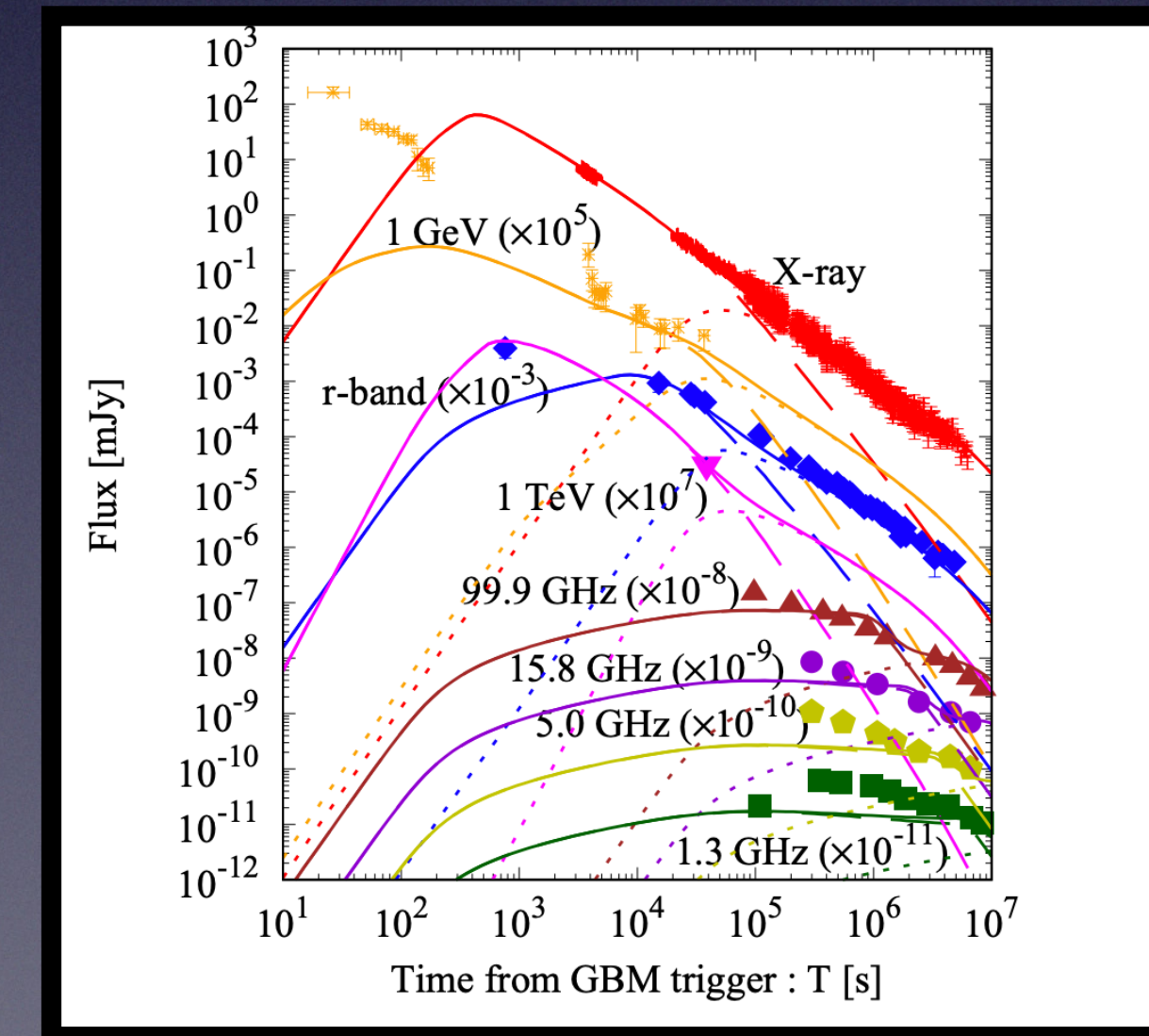
Top-hat jet model
From *Ren et al. (2023)*



Structured jet model
From *O'Connor et al. (2023)*



Single FS model
From *Laskar et al. (2023)*



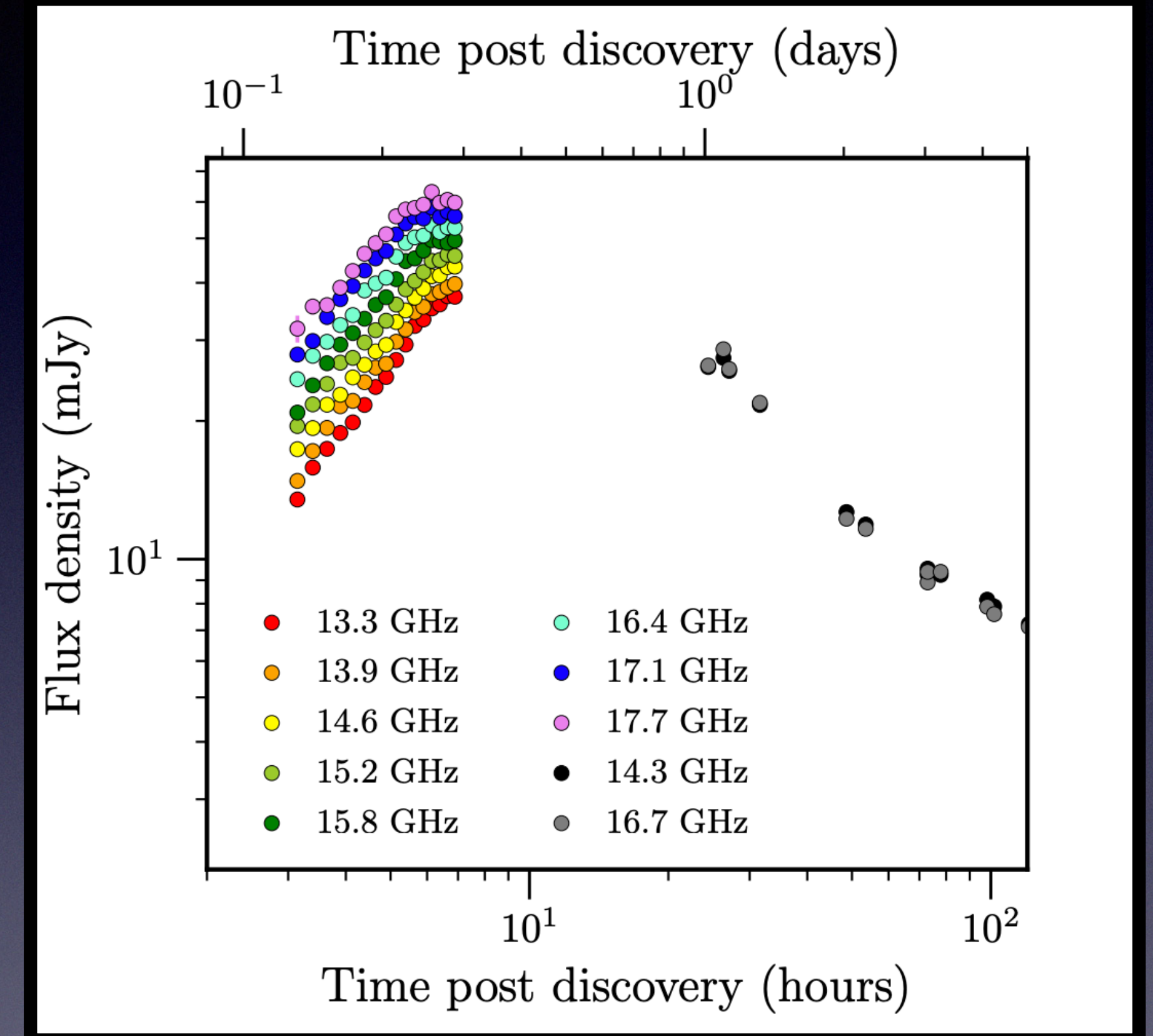
Two-component jet model
From *Sato et al. (2023)*

GRB 221009A

MWL Afterglow Models:

- (1) *Ren et al. (2023)*: top-hat jet in a wind-like environment
- (2) *Sato et al. (2023)*: two-component jet in a uniform environment
- (3) *Laskar et al. (2023)*: FS from a jet in a low-density wind-like environment
- (4) *O'Connor et al. (2023)*: structured jet in a medium with $k < 4/3$

...[See also *Gill & Granot (2023)*]



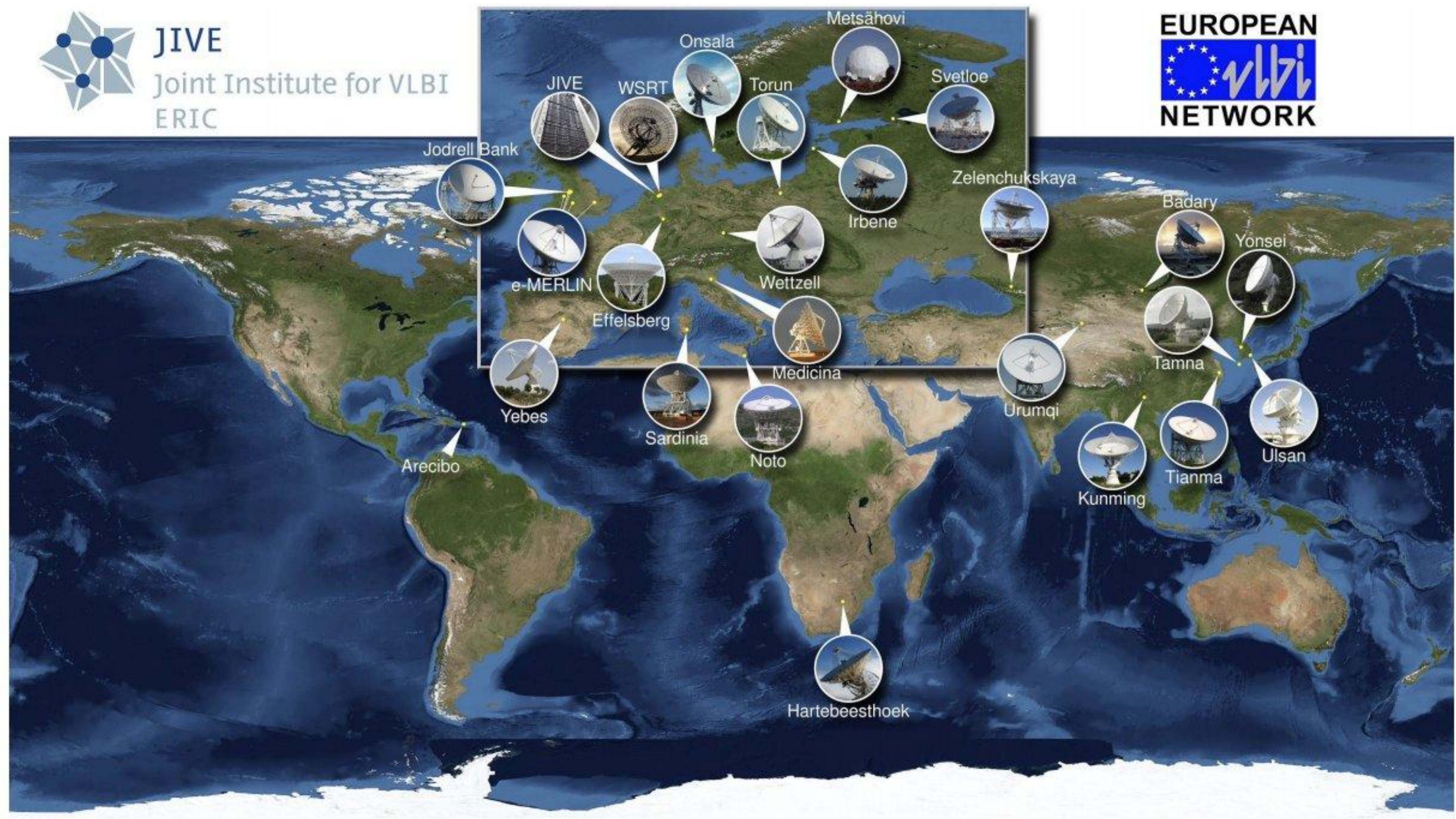
AMI observations of GRB221009A
From *Bright, Rhodes et al. (2023)*



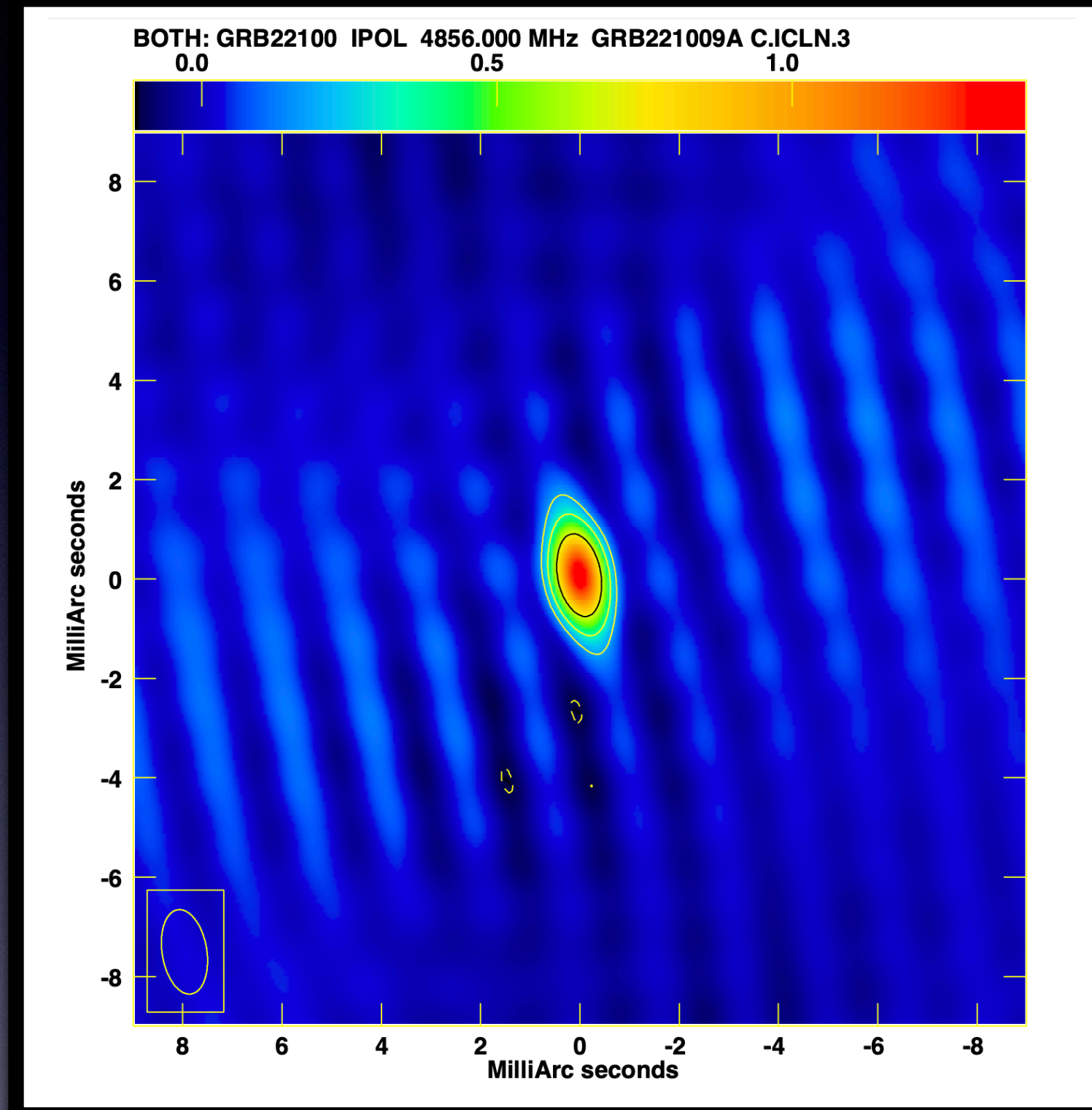
JIVE

Joint Institute for VLBI

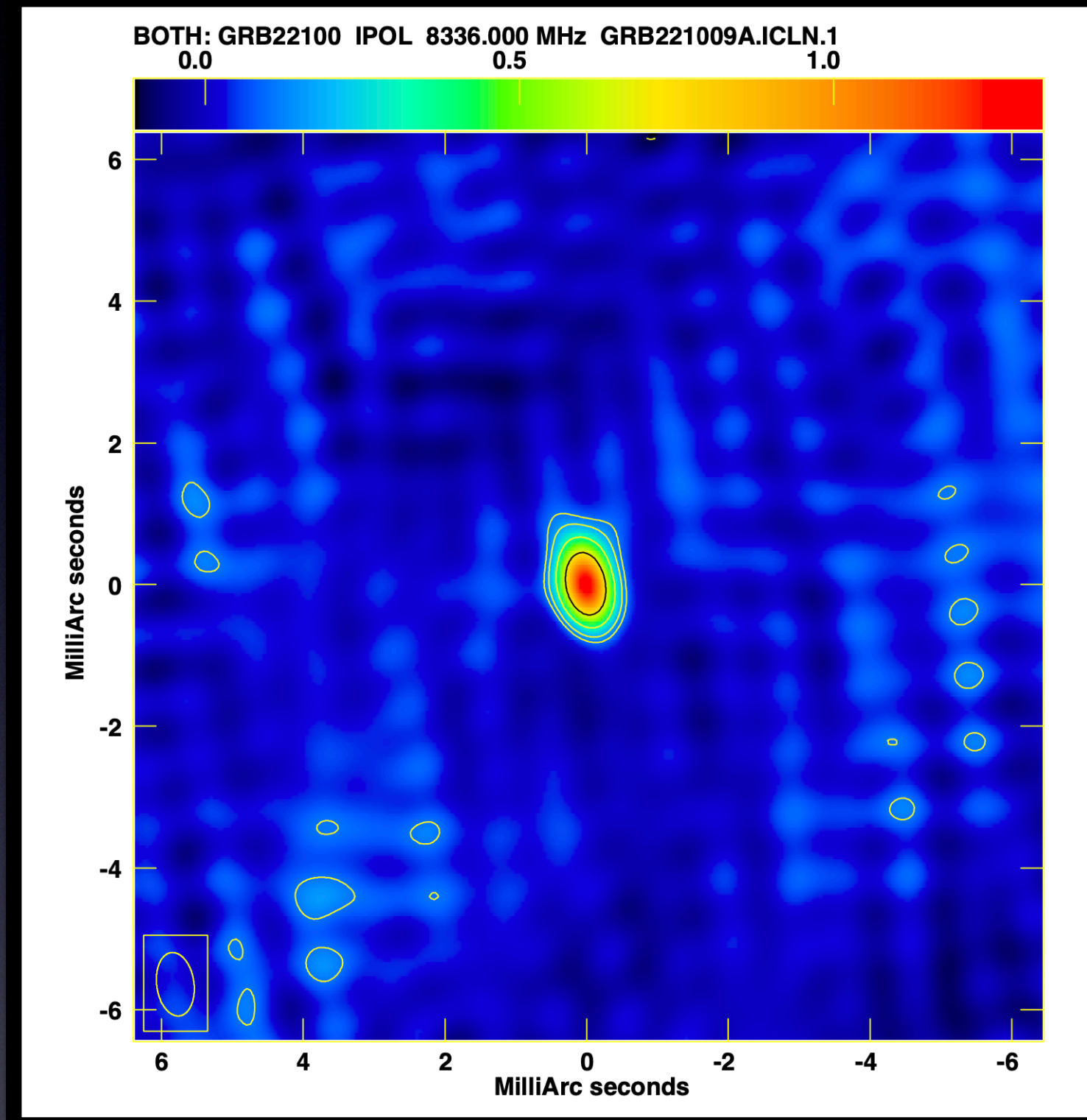
ERIC



GRB 221009A



EVN map of GRB221009A at 4.9 GHz.
The surface brightness peak is ~ 1.4 mJy/b.
The synthesized beam is 1.7×0.9 mas (PA = 9.25°).



EVN map of GRB221009A at 8.3 GHz.
The surface brightness peak is ~ 1.3 mJy/b.
The synthesized beam is 0.9×0.5 mas (PA = 7.7°).



**Global-VLBI
observation
planned for this
week!**



Outlook

The Square Kilometer Array



The Square Kilometer Array

Technical Information The Telescopes



The SKA telescopes are made up of arrays of antennas – SKA-mid observing mid to high frequencies and SKA-low observing low frequencies – to be spread over long distances. The SKA is to be constructed in phases: A first phase in South Africa and Australia, with a later expansion representing a significant increase in capabilities and expanding into other African countries, with the component in Australia also being expanded.

SKA1-Mid the SKA's mid-frequency telescope



Location: South Africa



Frequency range:
350 MHz
to
15.4 GHz
with a goal of 24 GHz



197 dishes
(including 64 MeerKAT dishes)



Maximum baseline:
150km

SKA1-Low the SKA's low-frequency telescope



Location: Australia



Frequency range:
50 MHz
to
350 MHz



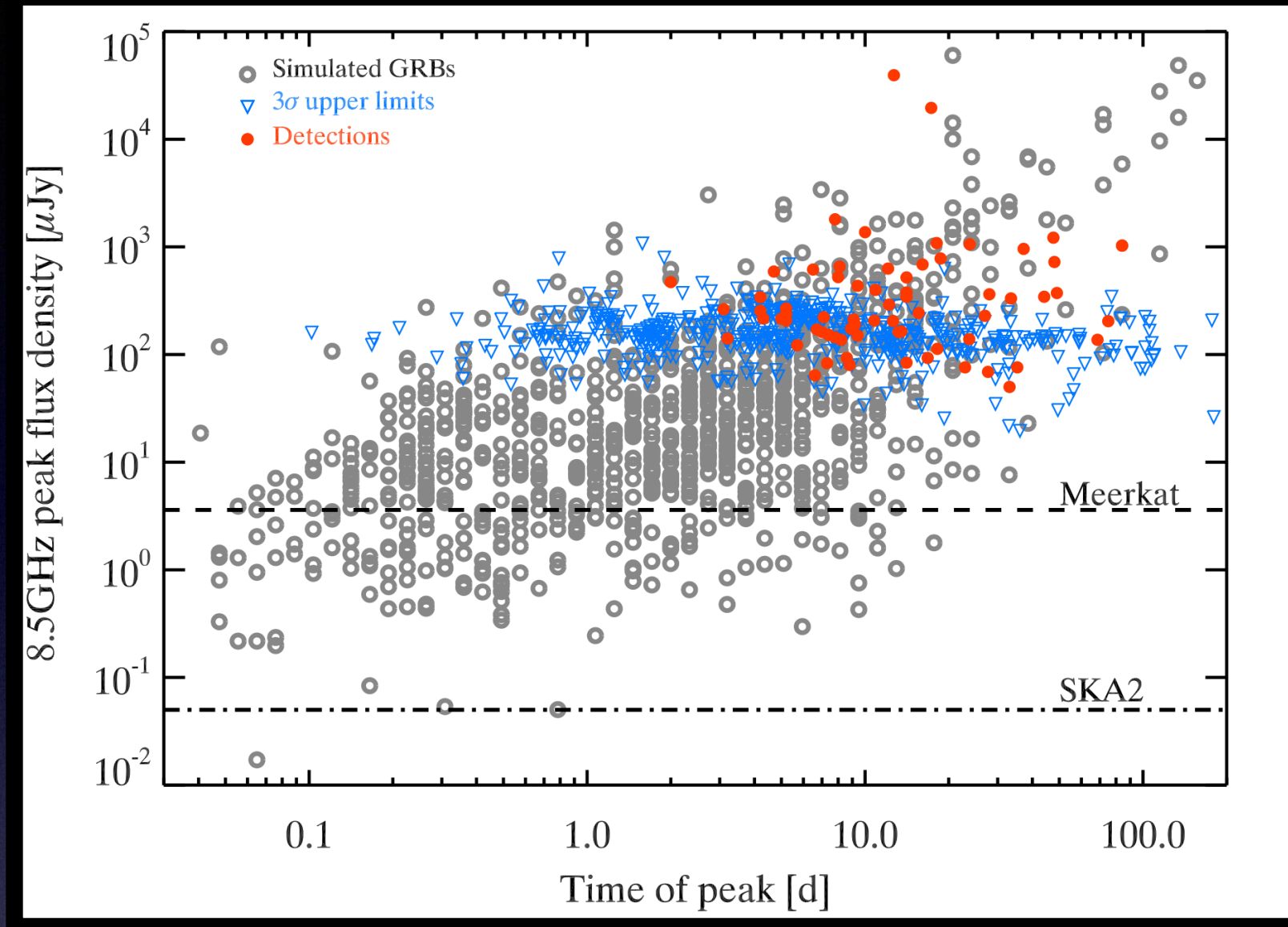
131,072
antennas spread between
512 stations



Maximum baseline:
~74km

SKA info sheet from the public SKAO website

SKA and GRBs

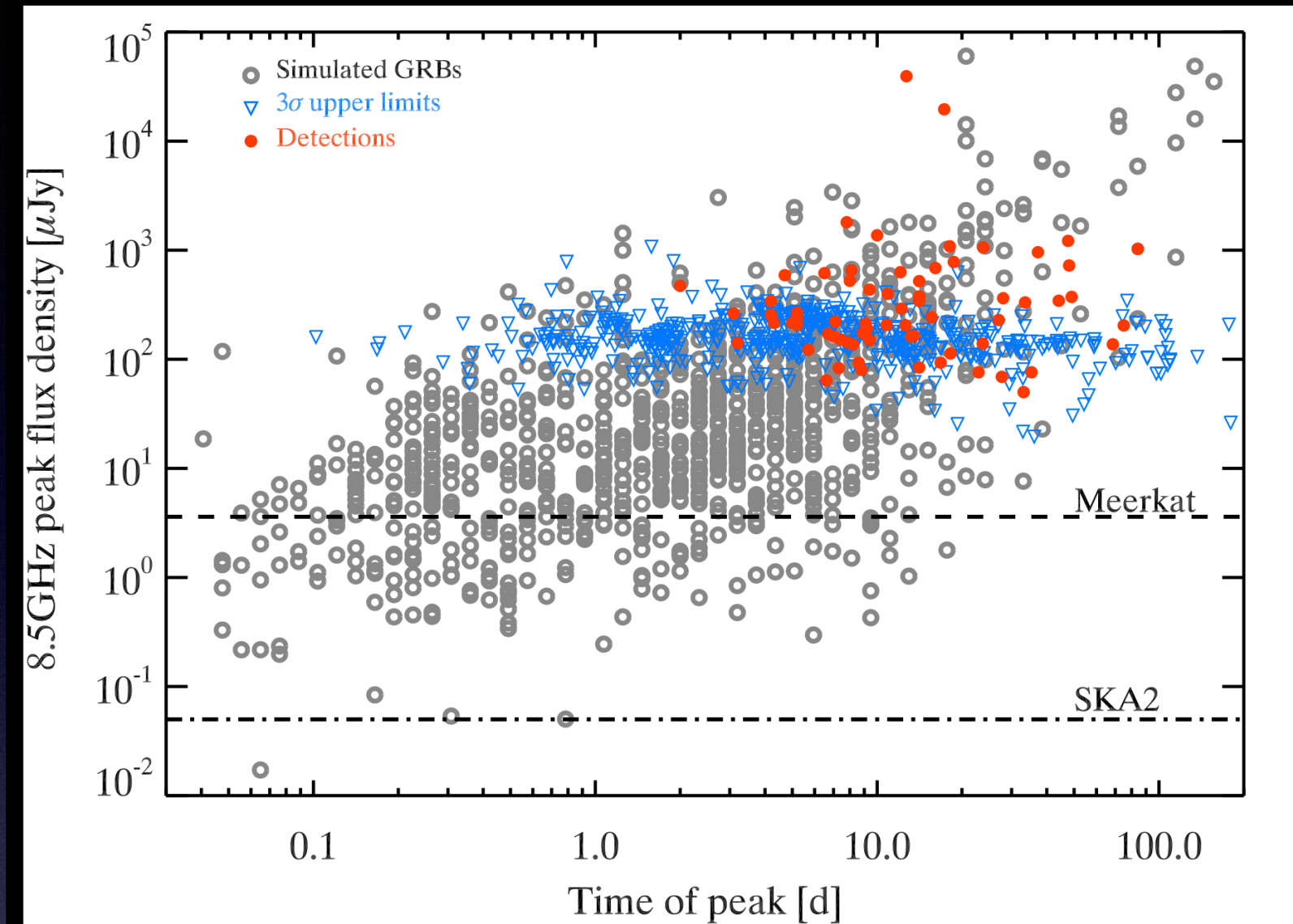


From 30% to almost 100% of detection rate



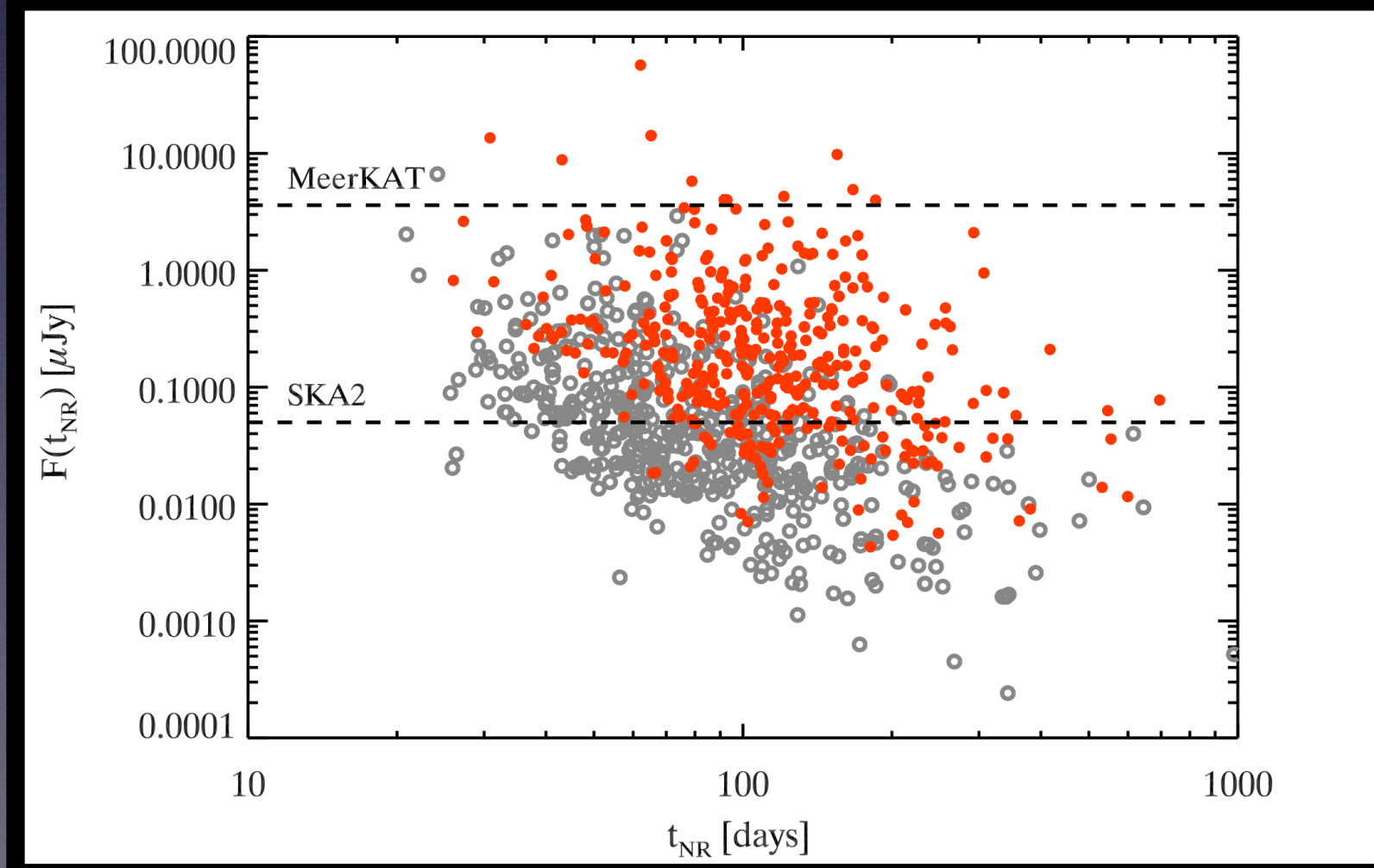
From Ghirlanda et al. (2013)

SKA and GRBs



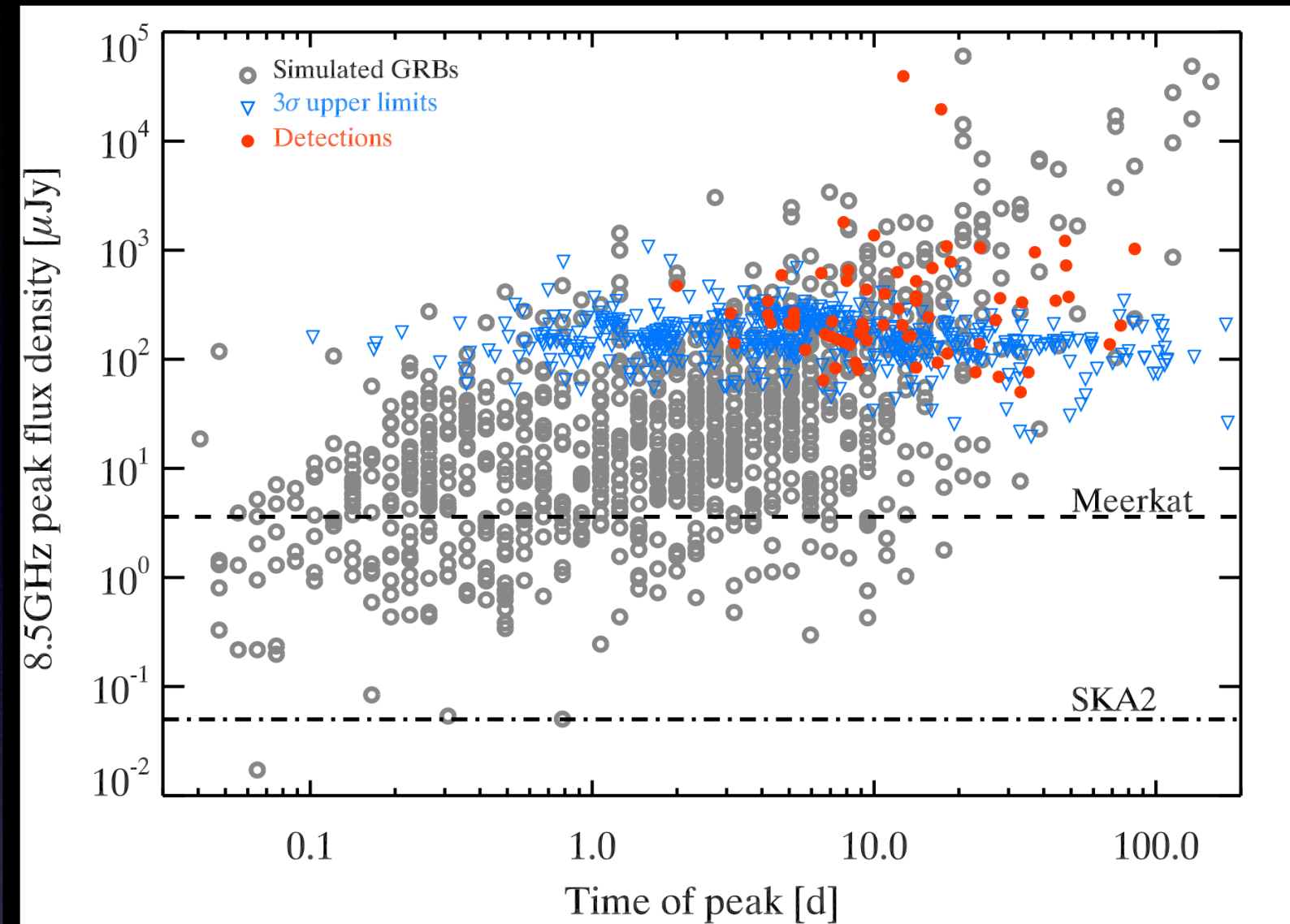
From 30% to almost 100% of detection rate

From <15% to almost 50% of detections at the transition time



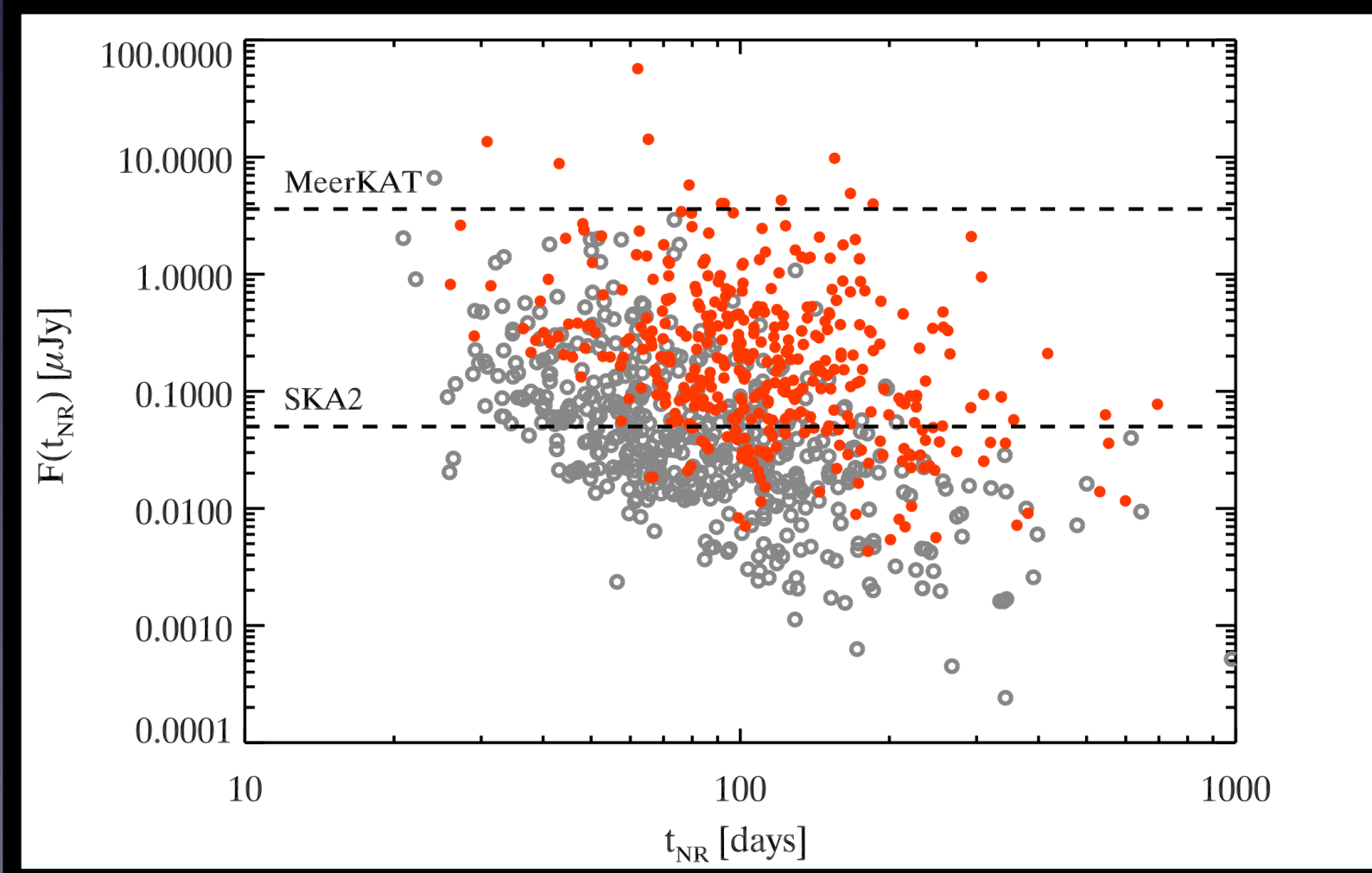
From Ghirlanda et al. (2013)

SKA and GRBs



From 30% to almost 100% of detection rate

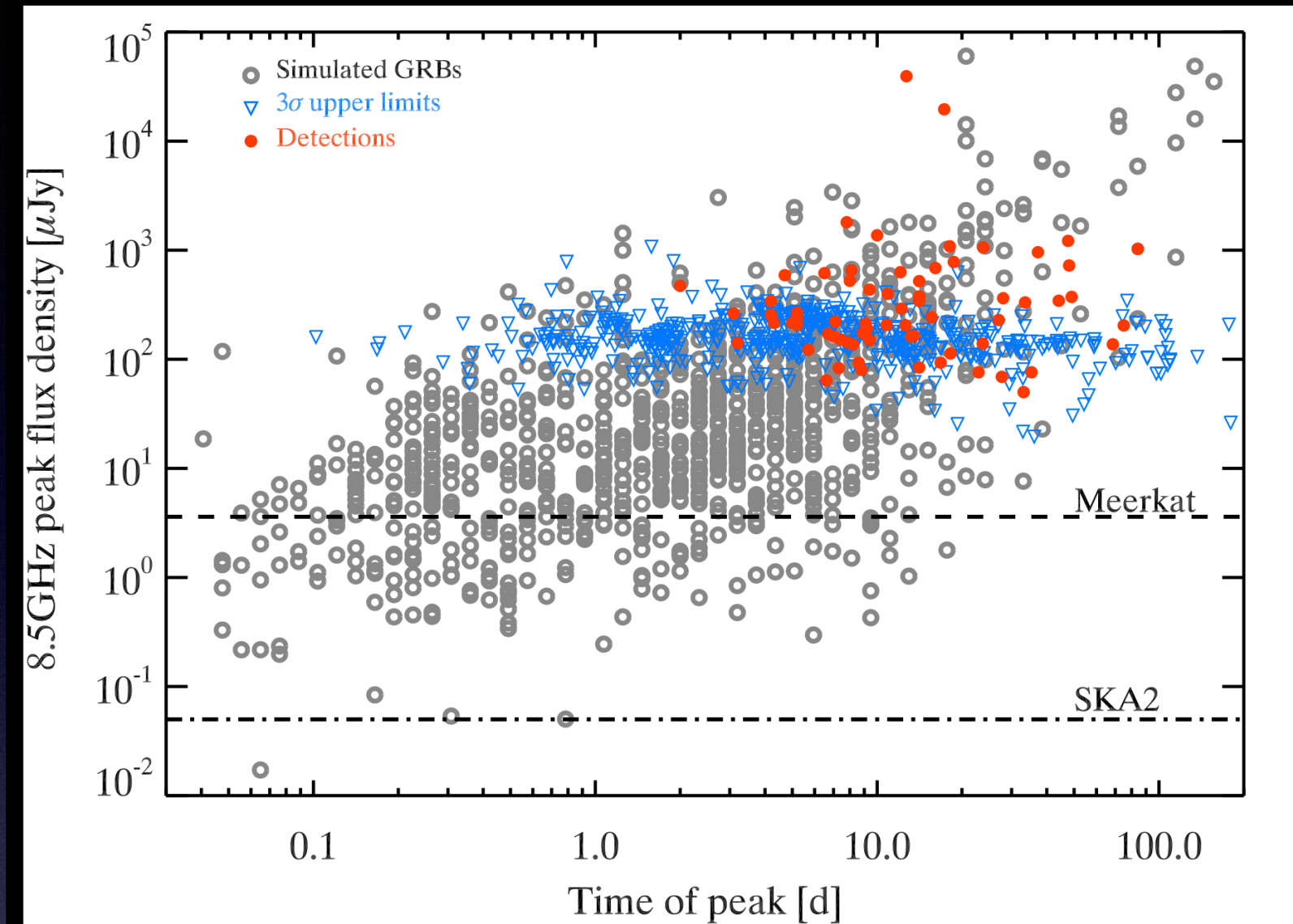
From <15% to almost 50% of detections at the transition time



+VLBI: structure and geometry

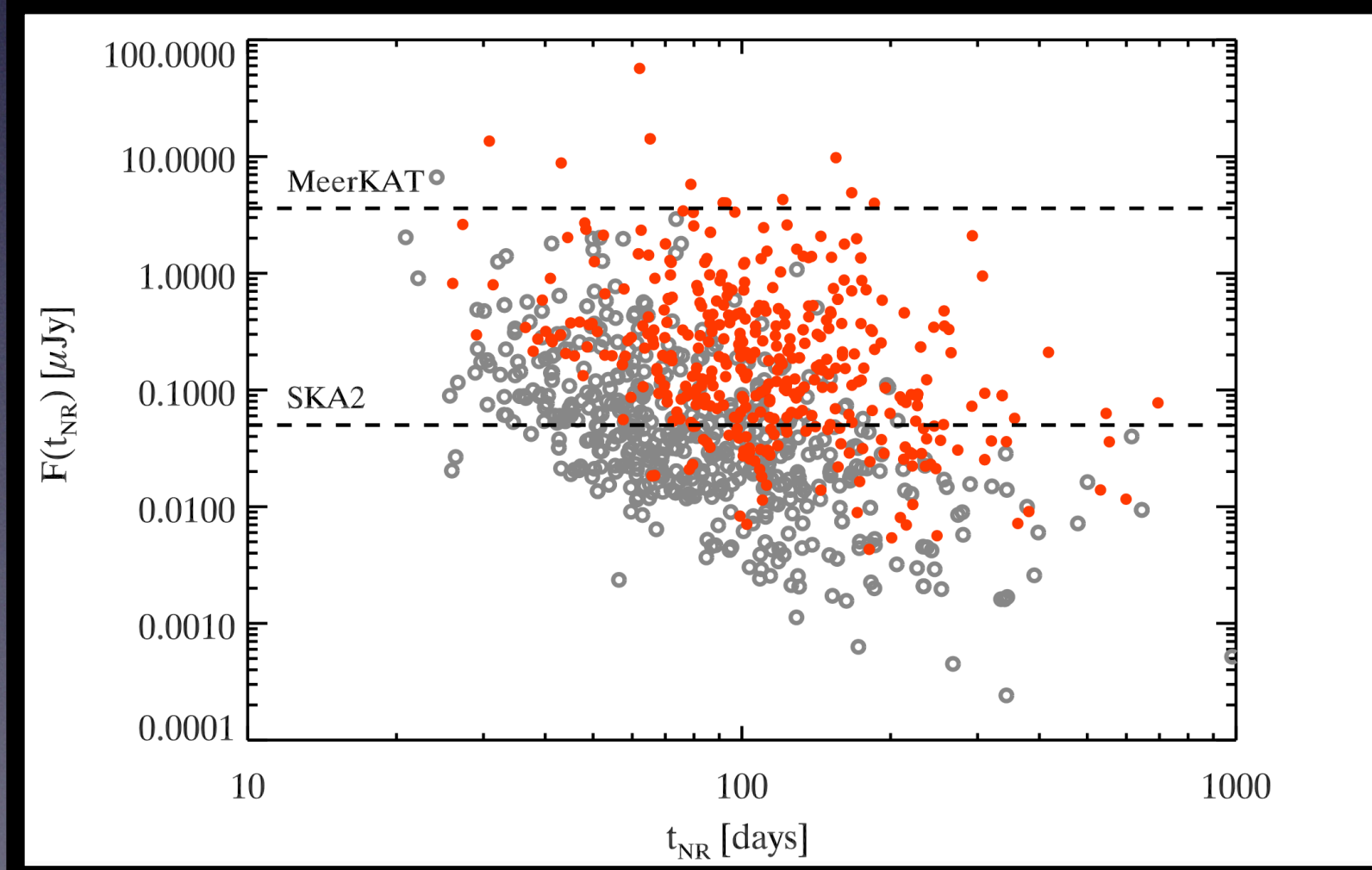
From Ghirlanda et al. (2013)

SKA and GRBs



From 30% to almost 100% of detection rate

From <15% to almost 50% of detections at the transition time

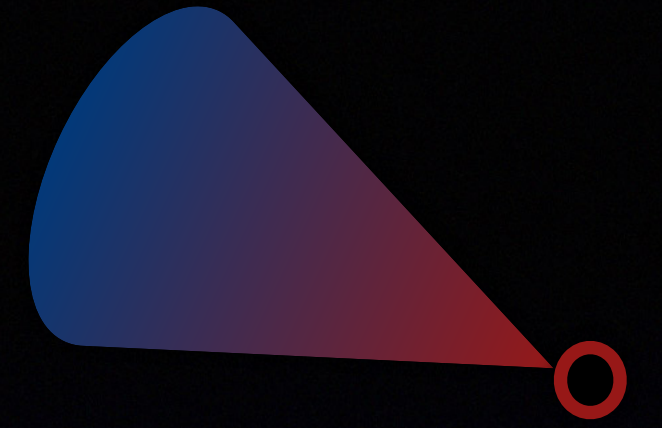


+**VLBI**: structure and geometry

...Unknown!

From Ghirlanda et al. (2013)

Conclusions



Radio observations can:

Break the **degeneracy** in the afterglow modeling

Reveal emitting **components** and/or mechanisms not accessible at other wavelengths

(with VLBI) provide a direct access on the **size** and the **geometry** of the afterglow

...SKA will enable this for the bulk of the GRB population!



Conclusions

Radio observations can:

Break the **degeneracy** in the afterglow modeling

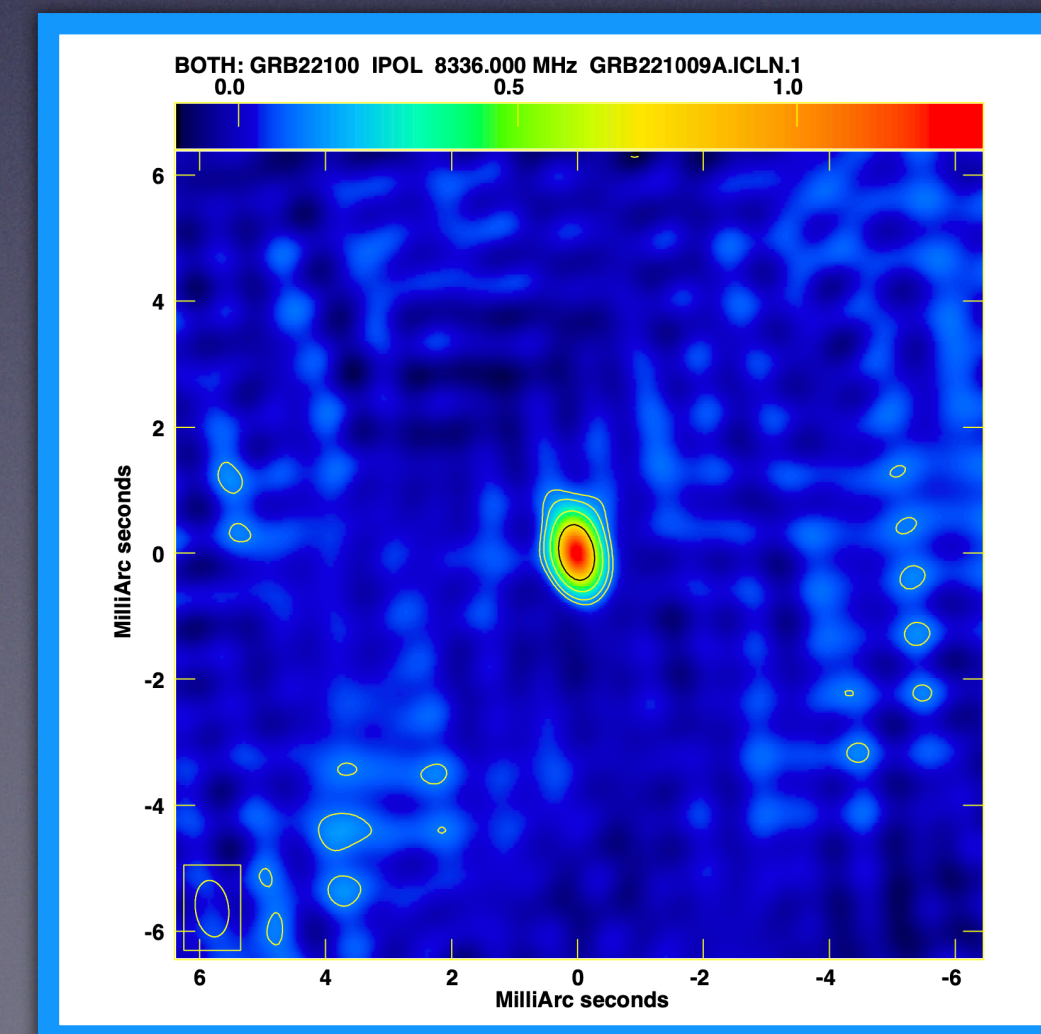
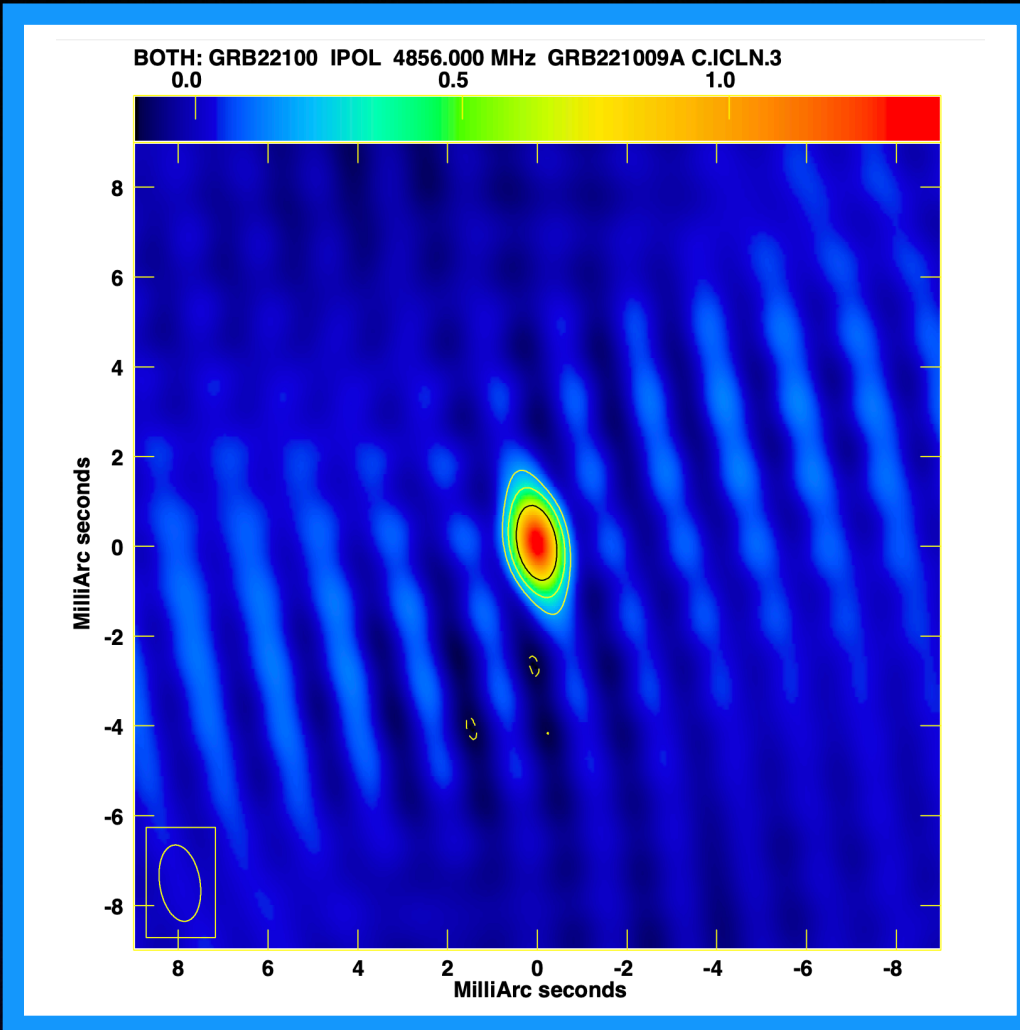
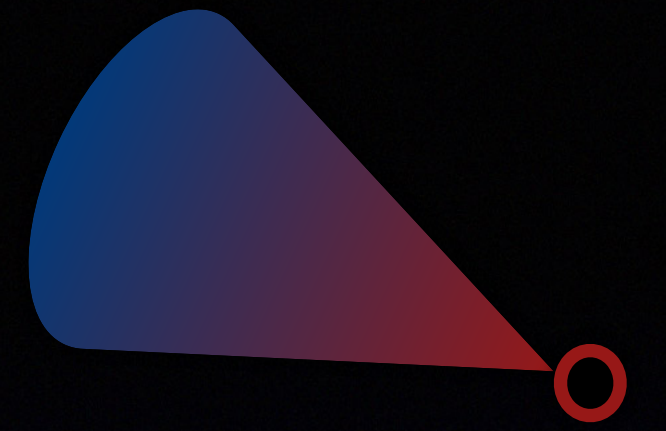
Reveal emitting **components** and/or mechanisms not accessible at other wavelengths

(with VLBI) provide a direct access on the **size** and the **geometry** of the afterglow

...SKA will enable this for the bulk of the GRB population!

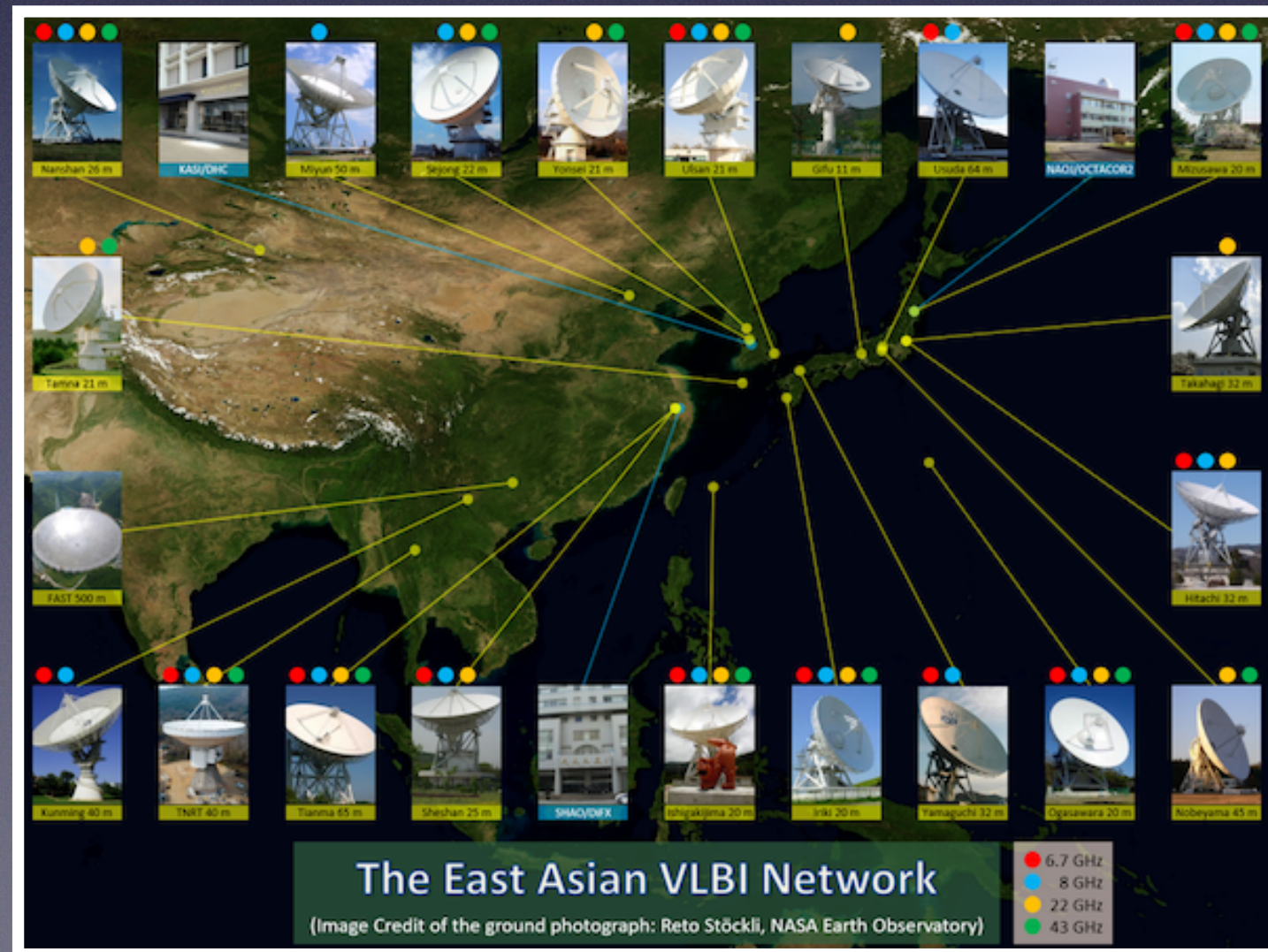
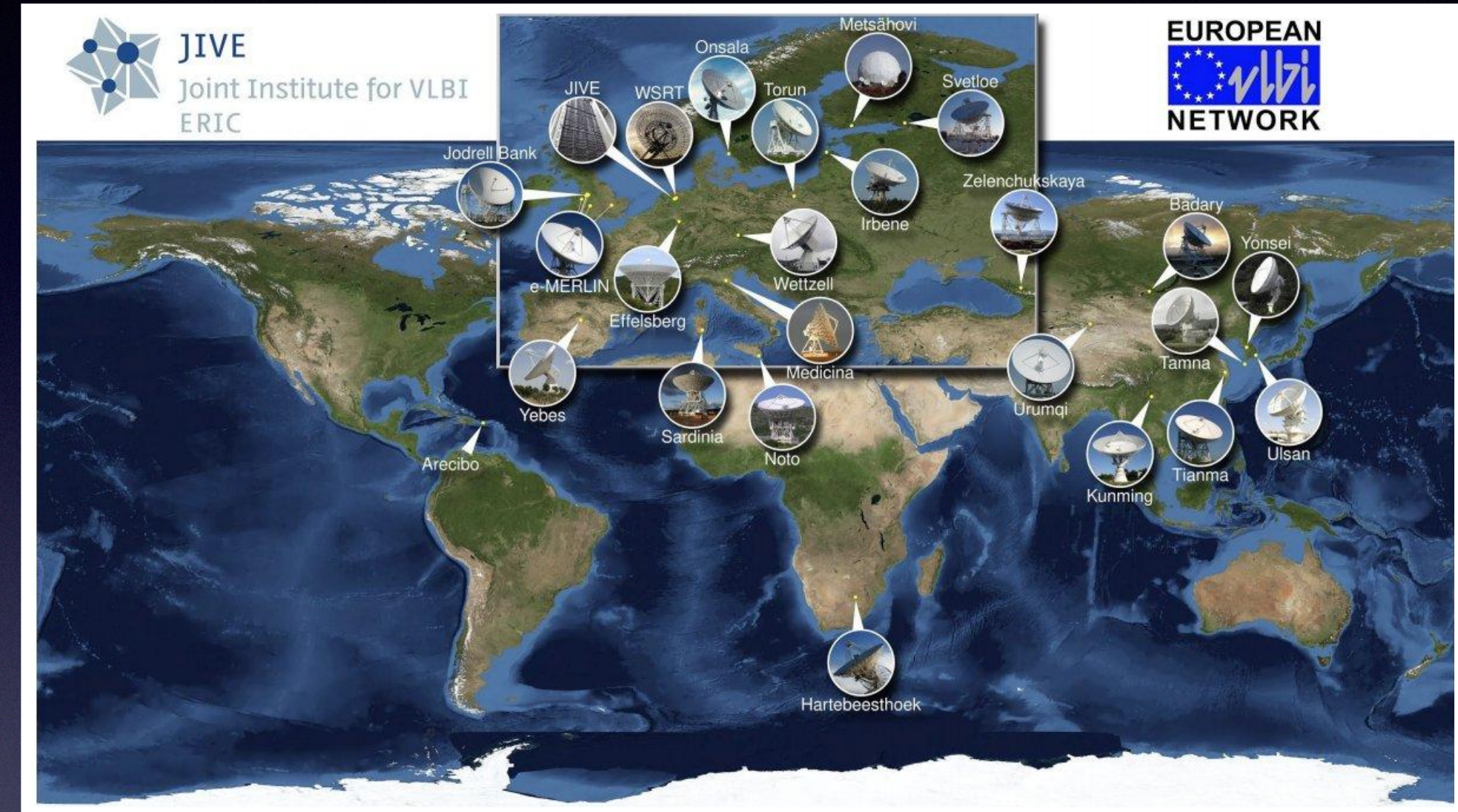
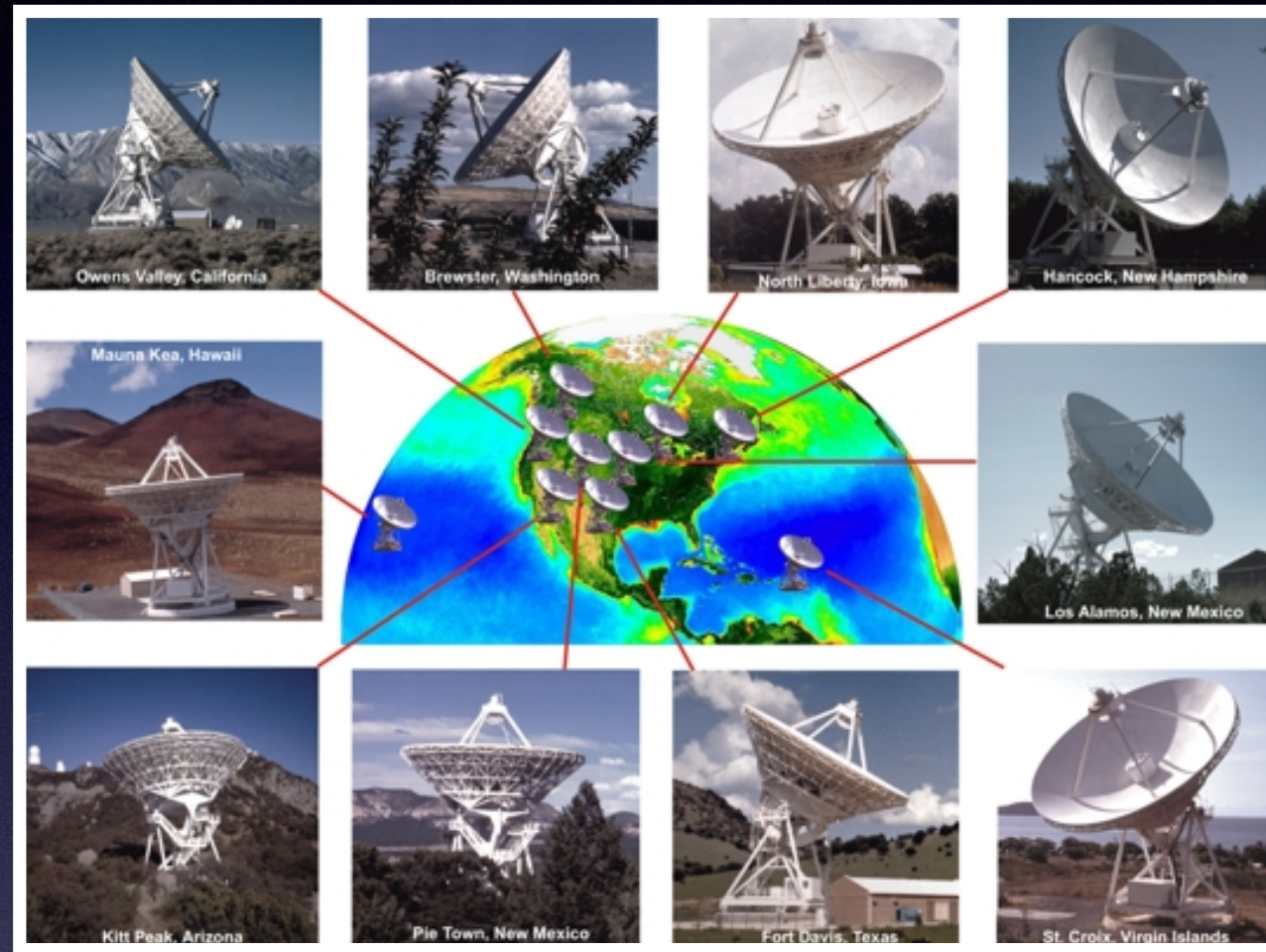
Take Home
Message

Radio is the key to study GRBs...
and VLBI can provide a unique view on
their dynamics and structure!



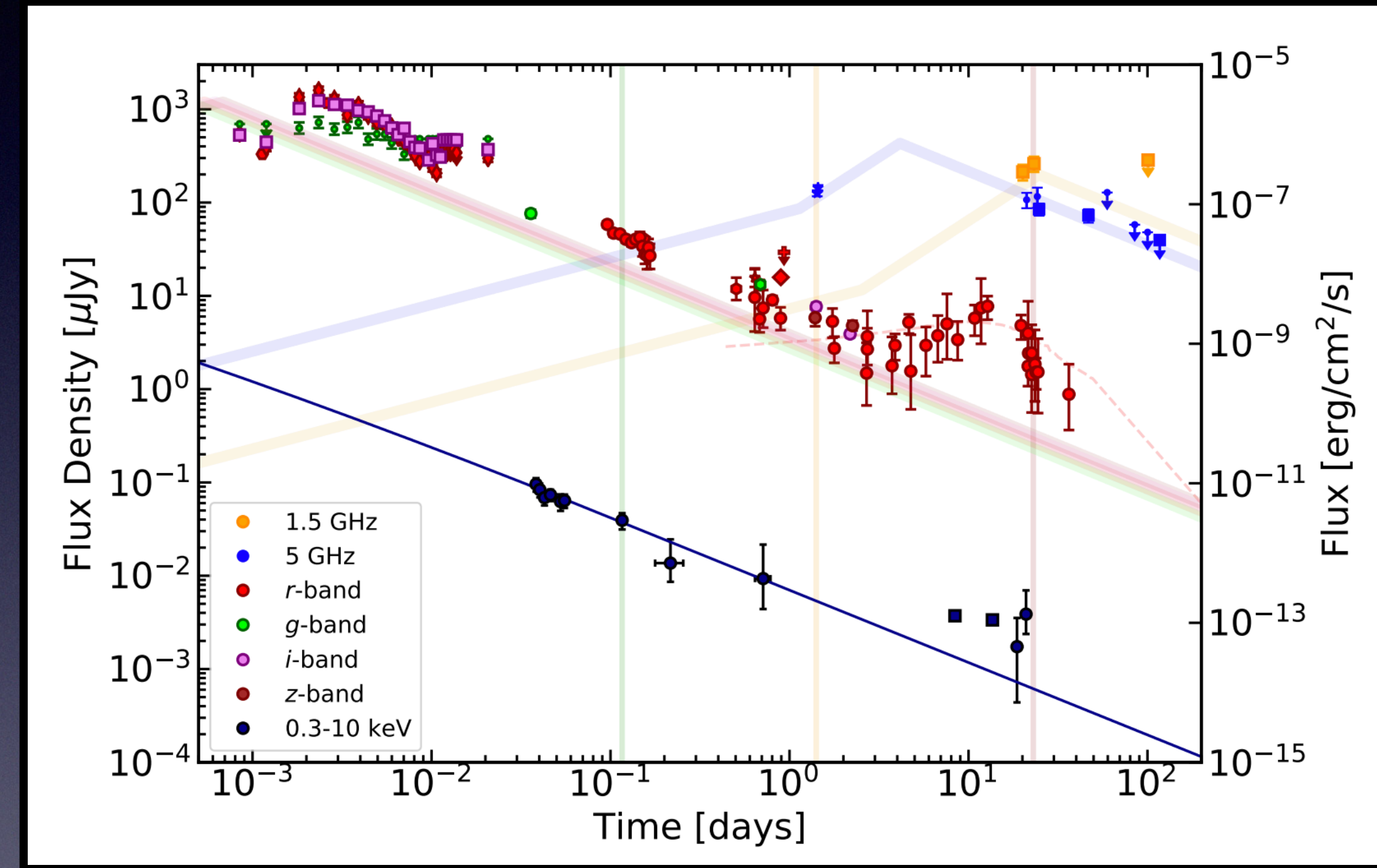
Backup Slides

Very Long Baseline Interferometry

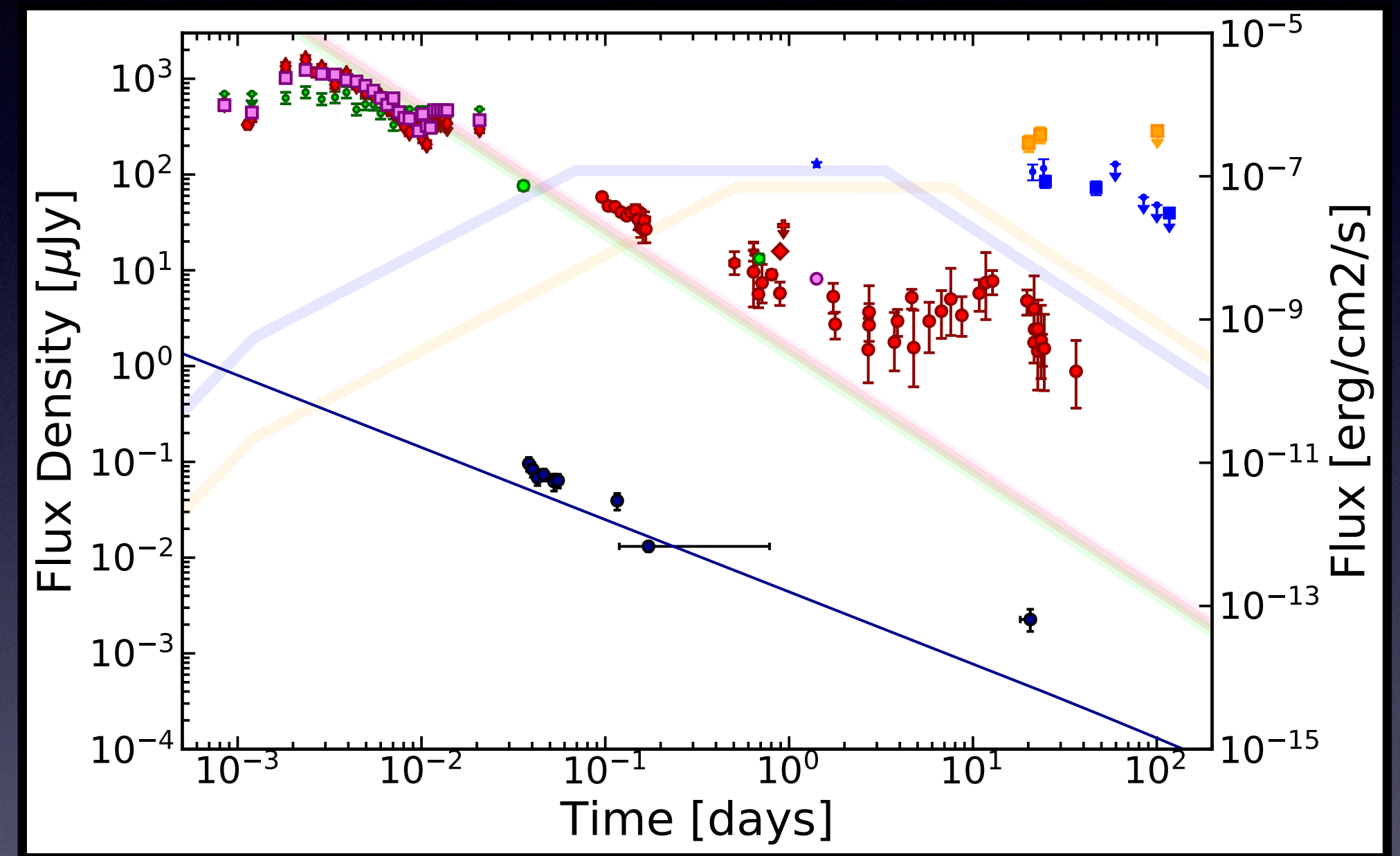
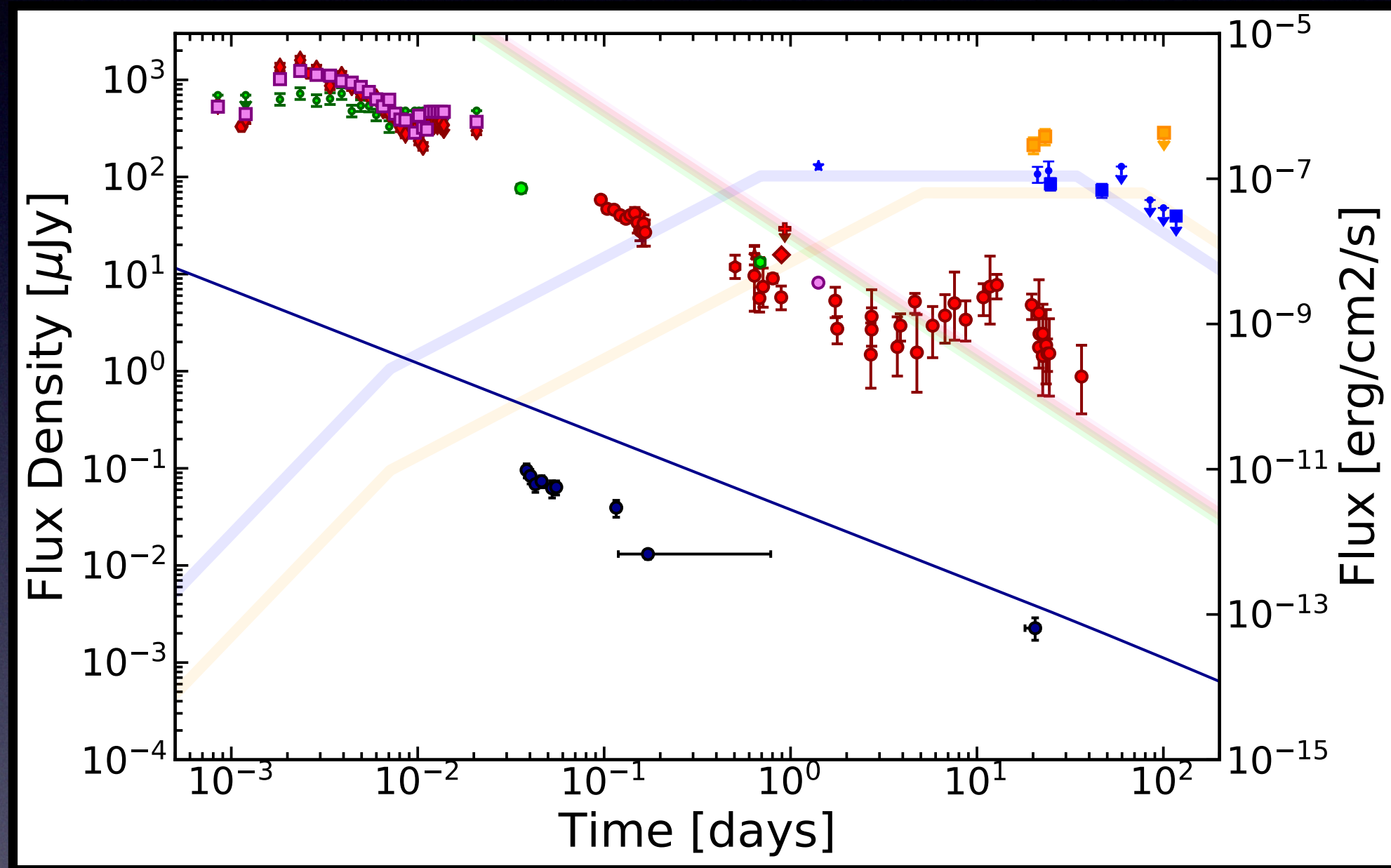


GRB 201015A

T - To [days]	Freq [GHz]	Peak [$\mu\text{Jy/b}$]	RMS [$\mu\text{Jy/b}$]	Array	Beam
1.4	4.23 - 7.10	132	5	VLA	1.70" x 1.14"
20	1.25 - 1.76	213	34	e-MERLIN	0.18" x 0.12
21	4.50 - 5.01	107	17	e-MERLIN	0.06" x 0.04"
23	1.25 - 1.76	261	40	e-MERLIN	0.19" x 0.12"
24	4.50 - 5.01	116	26	e-MERLIN	0.06" x 0.04"
25	4.57 - 5.11	85	9	EVN	1.8mas x 0.9mas
47	4.77 - 5.05	73	10	EVN	3.4mas x 2.8mas
60	6.55 - 7.06	-	43	e-MERLIN	0.12" x 0.07"
85	4.50 - 5.01	-	19	e-MERLIN	0.04" x 0.04"
100	4.50 - 5.01	-	16	e-MERLIN	0.07" x 0.03"
101	1.25 - 1.76	-	57	e-MERLIN	0.17" x 0.14"
117	4.77 - 5.05	-	13	EVN	3.1mas x 3.6mas



GRB 201015A



SKA and ngVLA

SKA1 Telescope Expected Performance – Imaging

Nominal frequency	110 MHz	300 MHz	770 MHz	1.4 GHz	6.7 GHz	12.5 GHz
Range [GHz]	0.05-0.35	0.05-0.35	0.35-1.05	0.95-1.76	4.6-8.5	8.3-15.4
Telescope	Low	Low	Mid	Mid	Mid	Mid
FoV [arcmin]	327	120	109	60	12.5	6.7
Max. resolution [arcsec]	9.7	3.5	0.7	0.3	0.06	0.03
Max. bandwidth [MHz]	300	300	700	810	3900	2 x 2500
Cont. rms, 1hr [μ Jy/beam] ^a	26	14	4.4	2	1.3	1.2
Line rms, 1hr [μ Jy/beam] ^b	1850	800	300	140	90	85
Resolution range for cont. & line rms [arcsec] ^c	12-600	6-300	1-145	0.6-78	0.13-17	0.07-9
Channel width (uniform resolution across max. bandwidth) [kHz]	5.4	5.4	13.4	13.4	80.6	80.6
Narrowest bandwidth, zoom mode [MHz]	3.9	3.9	3.1	3.1	3.1	3.1
Finest zoom channel width [Hz]	226	226	210	210	210	210

a. Continuum sensitivity at nominal frequency, assuming fractional bandwidth of $\Delta\nu/\nu = 0.3$

b. Line sensitivity at nominal frequency, assuming fractional bandwidth per channel of $\Delta\nu/\nu = 10^{-4}$ ($>10^{-6}$ will be possible)

c. The sensitivity numbers apply to the range of beam sizes listed
For more details refer to the document “Anticipated SKA1 Science Performance” (SKA-TEL-SKO-0000818 available on astronomers.skatelescope.org and at arxiv.org/abs/1912.12699)

SKA info sheet from the public SKAO website.

ngVLA Key Performance Metrics

Parameter [units]	2.4 GHz	8 GHz	16 GHz	27 GHz	41 GHz	93 GHz
Band Lower Frequency, f_L [GHz]	1.2	3.4	12.3	20.5	30.5	70.0
Band Upper Frequency, f_H [GHz]	3.5	12.3	20.5	34.0	50.5	116.0
Field of View FWHM [arcmin]	24.852	7.440	3.561	2.143	1.442	0.628
Aperture Efficiency [%]	0.828	0.936	0.941	0.920	0.886	0.648
Effective Area, $A_{\text{eff}} \times 10^3$ [m ²]	51.41	58.15	58.42	57.10	55.03	40.25
System Temp, T_{sys} [K]	17.07	22.00	24.40	32.42	47.41	65.37
Max Inst. Bandwidth [GHz]	2.3	8.8	8.2	13.5	20.0	20.0
Antenna SEFD [Jy]	232.3	264.8	292.2	397.3	602.8	1136.3
Resolution of Max. Baseline θ_{max} [mas]	2.97	0.89	0.43	0.26	0.17	0.08
Naturally Weighted Sensitivity						
Continuum rms, 1 hr [μ Jy/beam]	0.24	0.14	0.16	0.17	0.21	0.40

ngVLA expected performance. From the public ngVLA website.